Quantification of the spectral coupling of atmosphere and photovoltaic system performance: indexes, methods and impact on energy harvesting

Pedro M. Rodrigo[1*], Eduardo F. Fernández[2,**], Florencia M. Almonacid[2] and Pedro J. Pérez-Higueras[2]

[1]Universidad Panamericana, campus Aguascalientes, Facultad de Ingeniería, Josemaría Escrivá de Balaguer 101, Aguascalientes, Aguascalientes 20290, Mexico
[2]Centro de Estudios Avanzados en Energía y Medio Ambiente- Universidad de Jaén, s/n Las Lagunillas Campus, 23071 Jaén, Spain
[*]Corresponding author. Pedro M. Rodrigo, Tel: +52 449 910 6200, email: prodrigo@up.edu.mx
[**]Corresponding author. Eduardo F. Fernández, Tel: +34 953 21 3520, email: fenandez@ujaen.es

Abstract

Photovoltaic system performance is affected by changes in the input sunlight spectrum. Moreover, the different photovoltaic materials employed show different spectral responses, having different spectral behaviour as a result. Many authors have developed methods and proposed indexes for quantifying the spectral influences in photovoltaic systems under the time-varying weather variables. These methods use different equipment, different procedures and assumptions, present different levels of complexity and accuracy, and have advantages and disadvantages in each specific context and application. In this paper, for the first time, a systematic review of the available methods and photovoltaic spectral indexes is presented. Each alternative is analysed in detail and a comparative study is done. In addition, as several authors have measured and/or calculated the spectral impact on the energy yield of the different photovoltaic technologies at particular locations and climates, the existing results are summarized and discussed in order to elucidate the spectral behaviour of each technology as a function of the relevant atmospheric parameters, i.e. air mass, aerosol optical depth and precipitable water. The presented study covers non-concentrating and high-concentrating photovoltaic technologies and is intended for clarifying the methods available for the spectral analysis and the spectral impact on energy harvesting of the photovoltaic technologies.

Keyboards: photovoltaic devices, spectral characterization, mathematical procedures, outdoor performance

1. Introduction

A solar cell could be considered as a quantum converter based on the use of one or various semiconductor materials. The Spectral Response (SR) is widely accepted as the most relevant magnitude to understand the conversion of the incident photons into electricity of photovoltaic (PV) devices. It can be defined as the amperes generated per watt of incident light of a given wavelength. As an example, Fig. 1 shows the SR, also known as spectral absorption band, of some of the most wide-spread PV materials nowadays. At the same time, the energy of the photons received from the sun is distributed according to their different wavelengths, as given by the well-known Planck–Einstein relation: $E = h \cdot \nu = h \cdot c/\lambda$. The approximately constant energy distribution of the photons at the top of the atmosphere (TOA) of the planet Earth is affected through its pass over the atmosphere by different interaction physical phenomena. Hence, the wavelength distribution of the photons,

hereafter defined as spectral irradiance or spectral distribution, which reaches the Earth surface is inherently variable and different than the received at the TOA. As a result, the output of photovoltaic systems is going to be affected by the unavoidable spectral irradiance variations caused by the different attenuation processes produced in the atmosphere as a function of their different spectral abortion bands.

The changes in the input spectral distribution have demonstrated to play a relevant role on the electrical performance of PV systems under real operating conditions since early in the 1990s [1]. Bearing this in mind, the PV community has agreed a reference spectral distribution, or reference spectrum, to rate photovoltaic devices under the so-called standard test conditions (STC). This spectrum has been established by using different spectral models and from a rigorous study of the different extinction processes that occur in the atmosphere [2, 3, 4]. Nowadays, the most widely adopted spectral distribution to evaluate photovoltaic devices under STC is the ASTMG-173-03 reference spectrum provided by the American Society for Testing and Materials (ASTM) [5]. However, this spectrum rarely happens in outdoors where the main value of interest is not the efficiency under STC, but the electrical output under realistic operating conditions [6]. Because of this, the PV community has devoted big efforts in order to quantify and understand the impact of spectral changes on the output of the different solar devices developed over the last decades. This includes non-concentrating c-Si, a-Si, CIGS, CIS and CdTe [7, 8, 9, 10, 11], as well as non-concentrating dye-sensitized and perovskite [12, 13], and concentrating, lattice-matched and metamorphic-mismatched [14, 15], solar materials.

This papers aims to cover the most relevant studies concerning the spectral analysis of PV systems conducted within the last three decades. The review of the existing contributions reveals that different authors proposed different methods which use specific equipment and assumptions. While some authors have presented partial reviews of the state-of-the-art, nowadays there is not a systematic analysis of all of these procedures and it is not clear what the relations are between the different defined spectral indexes, what are the advantages and disadvantages of each one, and finally, what method is more convenient in each particular context and application. For instance, there are three recent works which include partial reviews of spectral indexes: Alonso-Abella et al. [16] cited some contributions regarding the “useful fraction”, the “spectral effective responsivity” and the “average photon energy” indexes for non-concentrating PV devices in order to introduce the method employed (“spectral factor”), but the reviewed methods are not defined in detail, neither compared and only a brief discussion on them can be found; Dirnberger et al. [17] made a historical overview of some articles focused on the spectral analysis of non-concentrating PV devices and mentioned the use of “average photon energy”, “useful fraction”, “integrated electric charge” and “spectral mismatch factor” as spectral indicators; Fernández et al. [15] focused on concentrating PV technologies and cited some works emphasizing the instruments used for the spectral characterization but not the methodologies employed. In general, authors present partial reviews focused on introducing their own methods but there is lack of a systematic and comprehensive study of the available methods and indexes for the different PV technologies. Moreover, the proposed indexes have not a unified nomenclature, and present different levels of complexity and accuracy which have not been discussed in many of the cases. So, there is confusion both in the PV researchers and developers when selecting the most suitable method for analysing the spectral influences in PV systems. In this paper, an in deep analysis on the available alternatives is conducted, supported by measurements and calculations

carried out by the authors. The aim is to provide a reference framework on the quantification of the spectral coupling of atmosphere and PV system performance for the future works of the PV community in this field.

The impact of this spectral coupling on the energy yield of PV systems has also been investigated by different authors in particular locations and climatic conditions for different PV materials. However, these contributions have not been analysed together and therefore general conclusions about the spectral impact on each PV technology have not yet been established. Moreover, the majority of these studies are based on pure experimental analyses and they usually lack a discussion of the fundamental phenomena involved in their findings by considering the weather variables at each site. This leads to a clear poorer understanding of the spectral performance of the different PV devices under the time-varying spectral changes. In this paper, the results available in the literature are summarized and discussed in order to elucidate the spectral behaviour of the different PV technologies as a function of the most relevant atmospheric parameters influencing the sunlight spectrum, i.e. air mass, aerosol optical depth and precipitable water. As will be shown, results provided by different researchers are consistent, in spite of using different methods and equipment, so that the general conclusions found will be of application in future solar cell development and PV system design.

The study is structured as follows: section 2 introduces the fundamentals of spectral solar radiation, presents the main atmospheric parameters and physical mechanisms which modify the solar spectrum that reaches the Earth surface and overviews the influence of changing spectra on the different PV materials; section 3 develops the review, classification, analysis and comparison of the spectral indexes and methods available in the literature; section 4 summarizes the annual spectral energy gain or loss values reported in the literature and draws the characteristic spectral behaviour of each PV technology as a function of the air mass, aerosol optical depth and precipitable water atmospheric parameters; finally, section 5 details the findings and conclusions of the research.

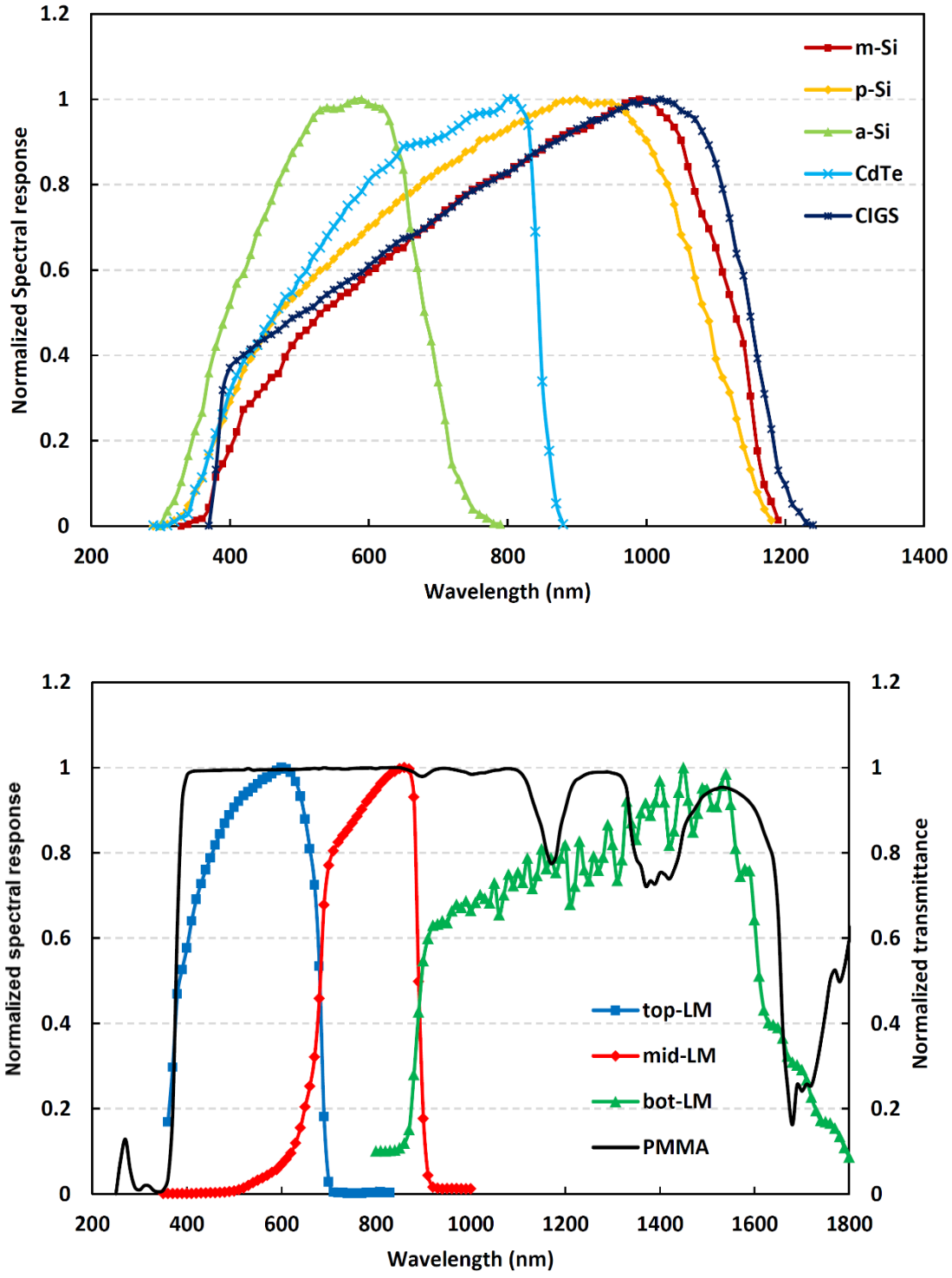

Fig. 1: Top: normalized spectral response of five kinds of PV materials: m-Si: mono-crystalline silicon; p-Si: poly-crystalline silicon; a-Si: amorphous silicon; CdTe: cadmium telluride; CIGS: copper indium gallium selenide. Bottom: normalized transmittance of a poly(methylmethacrylate) (PMMA) material and normalized spectral response of a triple-junction lattice-matched (LM) solar cell made up of: top junction: gallium indium phosphide (GaInP), middle junction: gallium indium

arsenide (GaInAs), bottom junction: germanium (Ge). The normalized spectral response and transmittance is the ratio of the spectral response/transmittance to the maximum value of the spectral response/transmittance for each material.

2. Spectral solar radiation

The Sun can be considered as a black body at a temperature of T ≈ 5770 K. According to the Stefan-Boltzmann´s law, $E = \sigma \cdot T^4$, and by considering the average radius of the Sun, $R_S \approx 6.96 \times 10^8$ m, and the distance from the sun to the planet Earth, $d_{S\text{-}E} \approx 1.496 \times 10^{11}$ m, the total radiation that reaches the TOA is approximately 1360 $W \cdot m^{-2}$. This value is usually defined as the solar constant (SC) and the wavelength irradiance distribution at the TOA as the extraterrestrial solar spectrum (E_{TR}). At the same time, the atmosphere acts as a filter that modifies the amount and spectral distribution of the E_{TR} spectrum by scattering and absorption phenomena. This attenuation depends on the amount of substance traversed by the solar rays in their course through the atmosphere and on the optical properties of the different atmospheric constituents (e.g. CH_4, O_2, CO_2, O_3, water vapour, aerosols, etc.). The spectral irradiance at the Earth´s surface (E_λ) can be described by the Beer–Lambert law: $E_\lambda = E_{TR} \cdot \exp\left(-\sum_i m \cdot \tau_{i,\lambda}\right)$, where $\tau_{i,\lambda}$ is the optical depth of each i-extinction process at a wavelength λ and m is the optical air mass. The optical air mass, or simply air mass (AM), quantifies the increase of the amount of substance traversed by the sun rays with respect to a vertical trajectory. Although each i-atmospheric constituent is going to have a specific value of AM, the air mass is usually reduced to a pure geometrical parameter function of the solar position whose minimum and maximum values are 1 (at a solar zenith angle of 0º) and 38 (at a solar zenith angle of 90º) [18]. A well-known formula for the air mass that accounts for the Earth´s sphericity was proposed by Gueymard [19]: $AM = \left[\cos\theta_z + 0.4835 \cdot \theta_z^{0.095846} / \left(96.7412 - \theta_z\right)^{1.754}\right]$, where θ_z is the Sun´s zenith angle. Aerosols are small particles suspended in the air either in solid or liquid state that scatter and absorb sunlight in a different extent depending of their size and optical properties. The attenuation of the spectral irradiance produced by the presence of aerosols in the atmosphere can be approximated by the Ångström turbidity formula: $AOD = AOD_{550} \cdot \left(\lambda / 0.55\right)^{-\alpha}$. In this equation, AOD is the aerosol optical depth, AOD_{550} is the amount of aerosols in a vertical column of the atmosphere at 550 nm and α is the Ångström or wavelength exponent [20]. The presence of water vapour in the atmosphere produces an important absorption effect on the spectral distribution reaching the Earth´s surface. The most widely used approach to quantify this effect is the so-called precipitable water (PW) that corresponds to the volume of liquid water that would be obtained if all the water vapour aloft was condensed [21]. Further information about the commented above can be found, for instance, in [22, 23, 24].

The three atmospheric parameters previously described (i.e. air mass, aerosol optical depth and precipitable water) are variable over space and time, and are widely considered as the most relevant to accurately evaluate the spectral impact on the electrical characteristics of photovoltaic devices [1, 25, 26]. Fig. 2 shows the influence of AM, AOD_{550} and PW in both the global and direct normal irradiance simulated with the Simple Model of the Atmospheric Radiative Transfer of Sunshine (SMARTS) [27]. Table 1 also shows the calculated attenuation on the ultraviolet (UV), UV-visible and near-infrared regions of the global and direct spectra produced by the variations of the values of

AM, AOD_{550} and PW plotted in Fig. 2. Based on Fig. 2 and Table 1, the main effects of each of these atmospheric parameters on the spectral irradiance are listed below:

- The increase of AM produces a strong attenuation on the ultraviolet (UV) region of the spectrum, and therefore, a red-shift of the spectral distribution.
- The increase of AOD_{550} produces a larger attenuation on the UV-visible region of the spectrum, and therefore, a red-shift of the spectral distribution. Moreover, the impact of AOD_{550} is larger in the direct normal irradiance than in the global irradiance since the aerosols scatter an important part of the incoming sunlight that is transformed into diffuse irradiance.
- The increase of PW produces a significant attenuation on the near-infrared region of the spectrum, and therefore, a blue-shift of the spectral distribution.

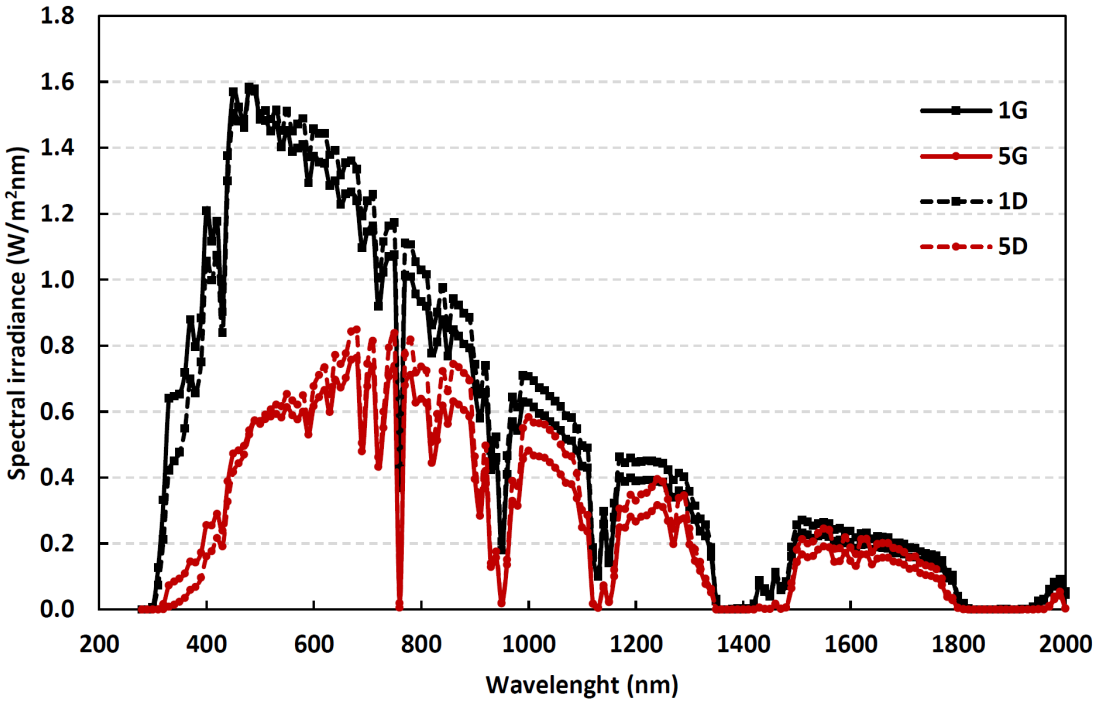
1.8
1.6
1.4
1.2
1.0
0.8
0.6
0.4
0.2
0.0
Spectral irradiance (W/m²nm)
200
400
600
800
1000
1200
1400
1600
1800
2000
Wavelenght (nm)
1G
5G
1D
5D

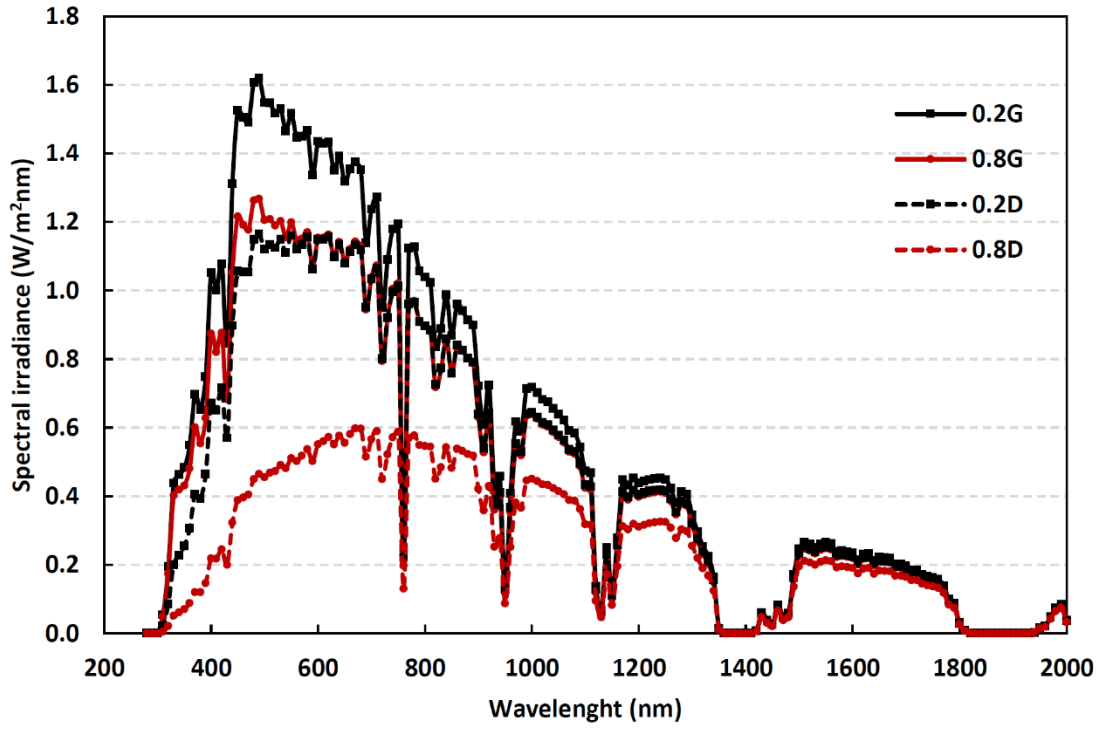
1.8
1.6
1.4
1.2
1.0
0.8
0.6
0.4
0.2
0.0
Spectral irradiance (W/m²nm)
200
400
600
800
1000
1200
1400
1600
1800
2000
Wavelenght (nm)
0.2G
0.8G
0.2D
0.8D

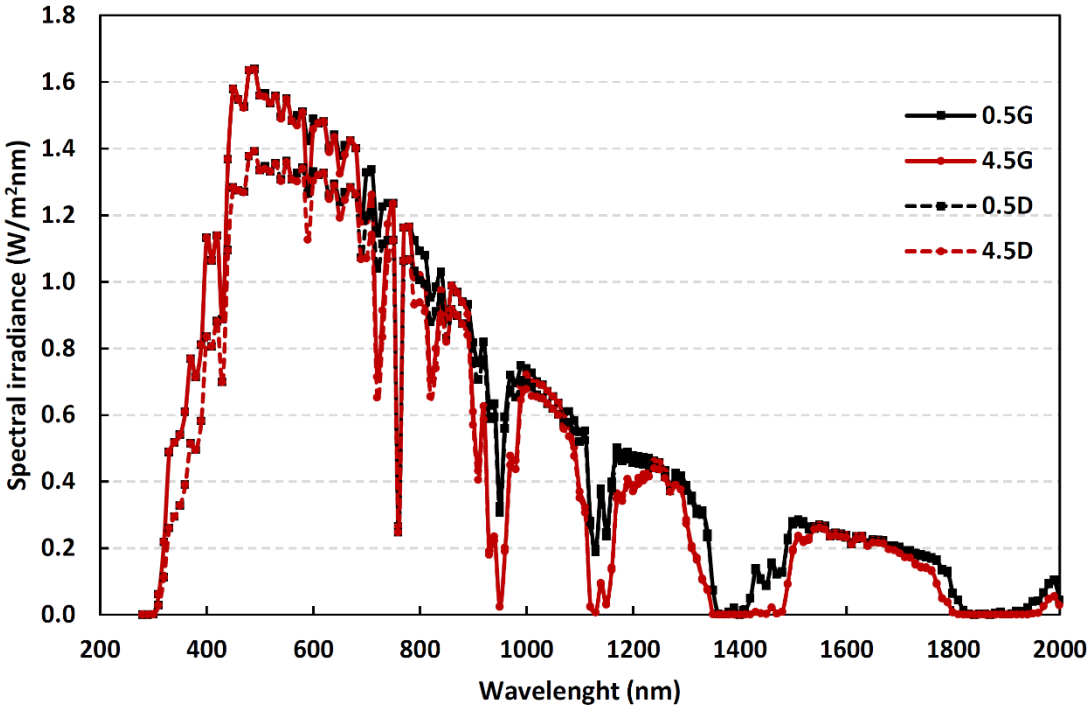

Fig. 2: Impact on the global (denoted as G) and direct (denoted as D) spectral irradiance due to air mass (top), aerosol optical depth at 550 nm (middle) and precipitable water (bottom) simulated with the SMARTS model. The values of the changing parameters are indicated in the legend of each graph. The other parameters are kept constant at the reference values defined by the AM1.5d ASTMG-173-03 reference spectrum (i.e. AM = 1.5, AOD_{550} = 0.084, PW = 1.42cm).

Table 1
Attenuation on the ultraviolet (UV), UV-visible and near-infrared regions of the global and direct spectra produced by the variations of the values of air mass (AM), aerosol optical depth at 550 nm (AOD_{550}) and precipitable water (PW) plotted in Fig. 2.

	Direct			**Global**		
	AM	**AOD_{550}**	**PW (cm)**	**AM**	**AOD_{550}**	**PW (cm)**
UV	91%	70%	0%	84%	14%	0%
UV-visible	59%	55%	3%	60%	19%	3%
Near-infrared	30%	27%	21%	35%	10%	21%

Based on the above, it is evident that the variations of each atmospheric parameter will produce different effects on the performance of photovoltaic devices depending on their absorption bands. The individual impact of these atmospheric parameters on the performance of different photovoltaic materials has been previously investigated in [15, 13, 12, 28], and is also shown in Fig. 3. Based on these previous studies and in the sensitivity analysis plotted in Fig. 3, the following main conclusions can be reached:

- High concentrator photovoltaic (HCPV) technology is more affected by the spectral changes than conventional PV technology. This is mainly due to the use of multi-junction solar cells

based on the in-series connection of subcells with different energy gaps, as well as the optical elements used to concentrate the sunlight.

- The AM is the parameter with the largest impact on the performance of photovoltaic devices. Materials with high energy gap are more affected, while materials with low energy gap show a more stable behaviour.
- The AOD is the second parameter with the strongest impact on the performance of photovoltaic devices. As in the previous case, the materials with high energy gap are more affected than materials with low energy gap. Also, the AOD produces a lower impact on the performance of PV than HCPV technology, due to the lower effect of AOD in the global component of the radiation.
- The PW is the third parameter with the largest impact on the performance of PV devices. Once again, the materials with high energy gap are more affected than materials with low energy gap.

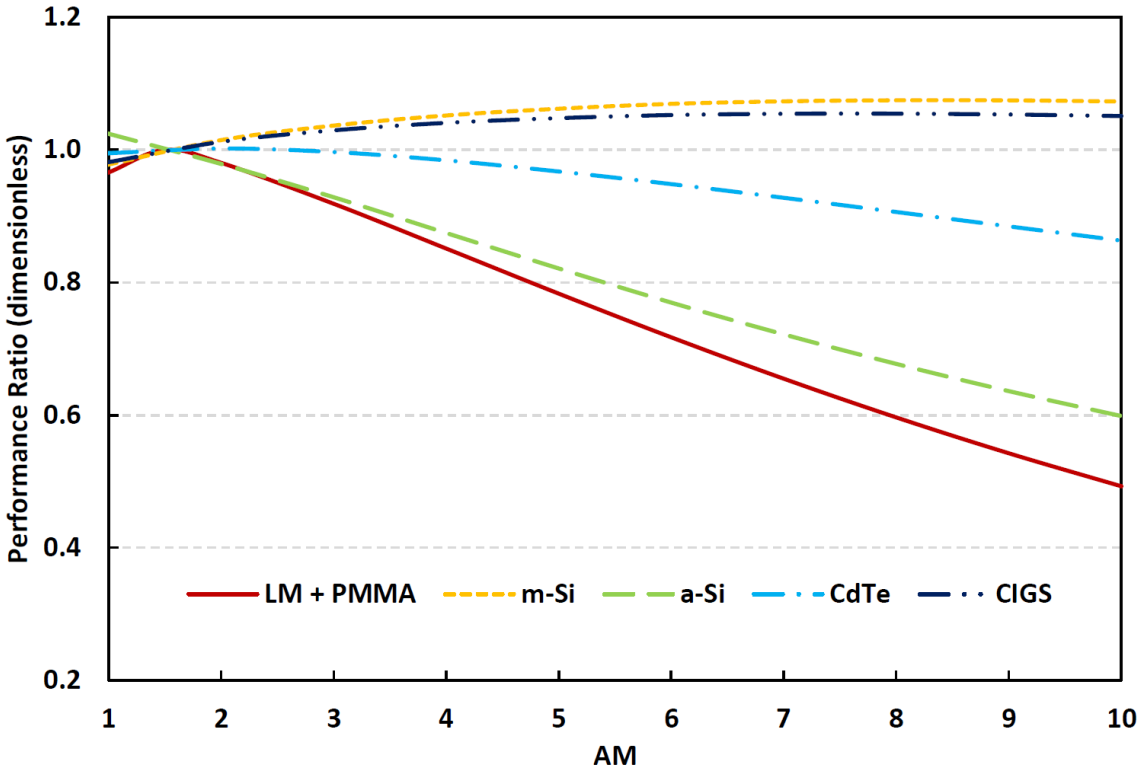

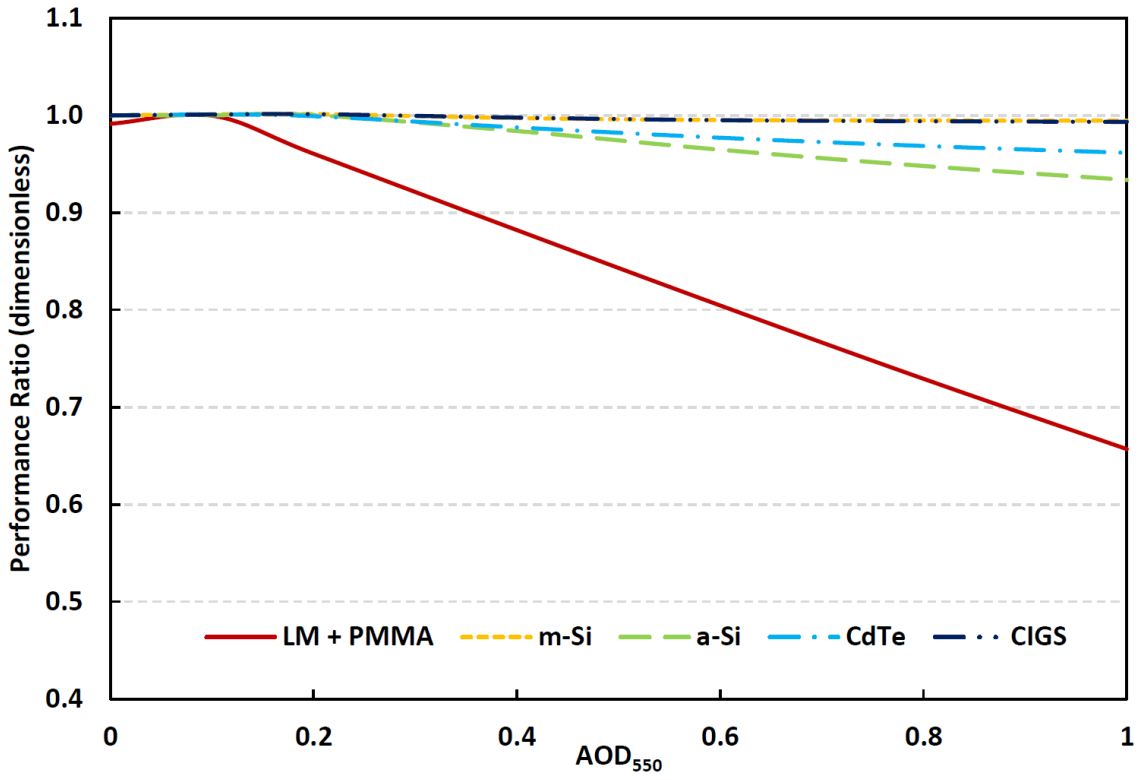
1.1
1.0
0.9
0.8
0.7
0.6
0.5
0.4
Performance Ratio (dimensionless)
LM + PMMA
m-Si
a-Si
CdTe
CIGS
0
0.2
0.4
0.6
0.8
1
AOD550

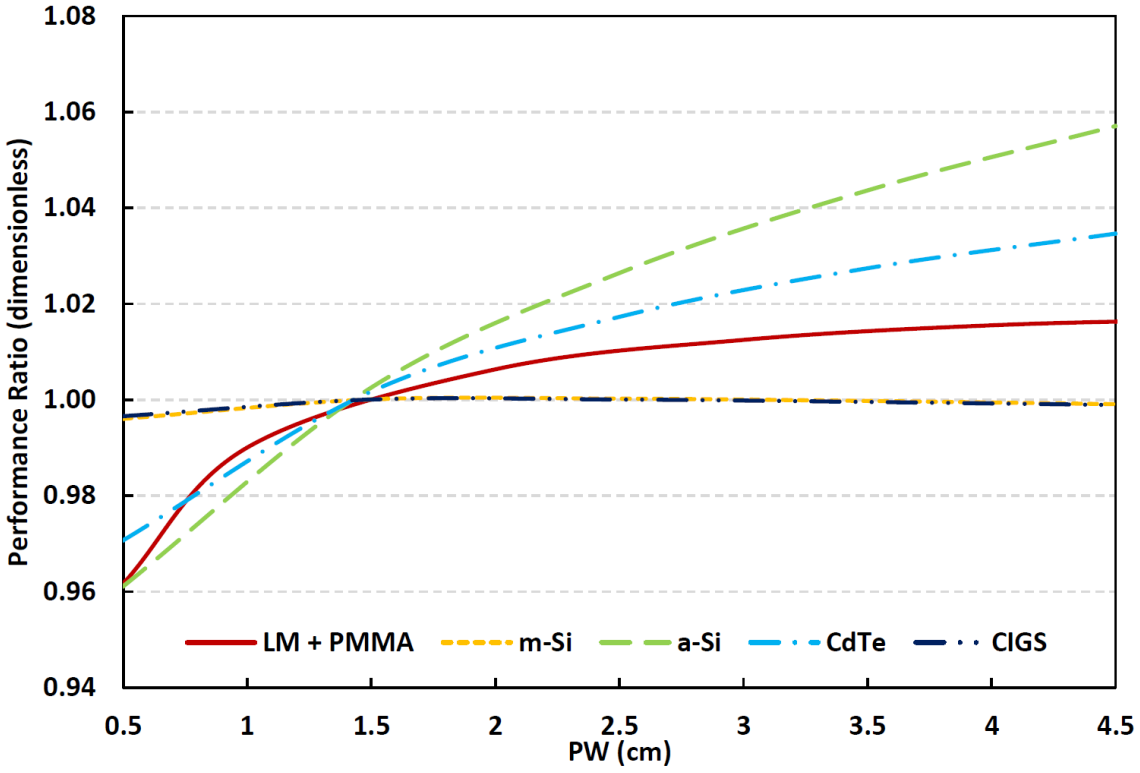
1.08
1.06
1.04
1.02
1.00
0.98
0.96
0.94
Performance Ratio (dimensionless)
LM + PMMA
m-Si
a-Si
CdTe
CIGS
0.5
1
1.5
2
2.5
3
3.5
4
4.5
PW (cm)

Fig. 3: Individual impact of air mass (top), aerosol optical depth at 550 nm (middle) and precipitable water (bottom) on the performance of various PV technologies simulated with the SMARTS model following the procedure described in [15, 13, 12, 28]. The spectral response of each material can be found in Fig. 1. The other parameters are kept constant at the reference values defined by the AM1.5d ASTMG-173-03 reference spectrum (i.e. AM = 1.5, AOD_{550} = 0.084, PW = 1.42 cm). The spectral Performance Ratio in the y-axis represents the quotient between the maximum power of the device only accounting for irradiance and spectral effects and the ideal maximum power only accounting for irradiance effects.

3. Review of spectral indexes

In this section, a review of spectral indexes is presented. The indexes have been classified into PV device-independent indexes and PV device-dependent indexes. PV device-independent indexes do not make use of any physical characteristics of a PV device while PV device-dependent indexes do. The PV device-dependent indexes have been further classified according to three categories: indexes that characterize the spectral impact on a PV device, indexes that characterize the relative spectral impact between two PV devices, and indexes that characterize the spectrum from multi-junction solar cells. These categories identify the main use of the indexes. In the first category, non-concentrating PV devices and HCPV devices are differentiated. As we could not find spectral studies concerning low-concentrating and medium-concentrating photovoltaic devices, these kinds of devices have not been included in the classification. Fig. 4 shows the reviewed spectral indexes grouped according to this classification. Many of these indexes are actually several indexes including instantaneous indexes and/or energetic indexes over a period of time with very similar meanings and definitions. The following subsections define and summarize the main characteristics of the spectral indexes according to the proposed classification.

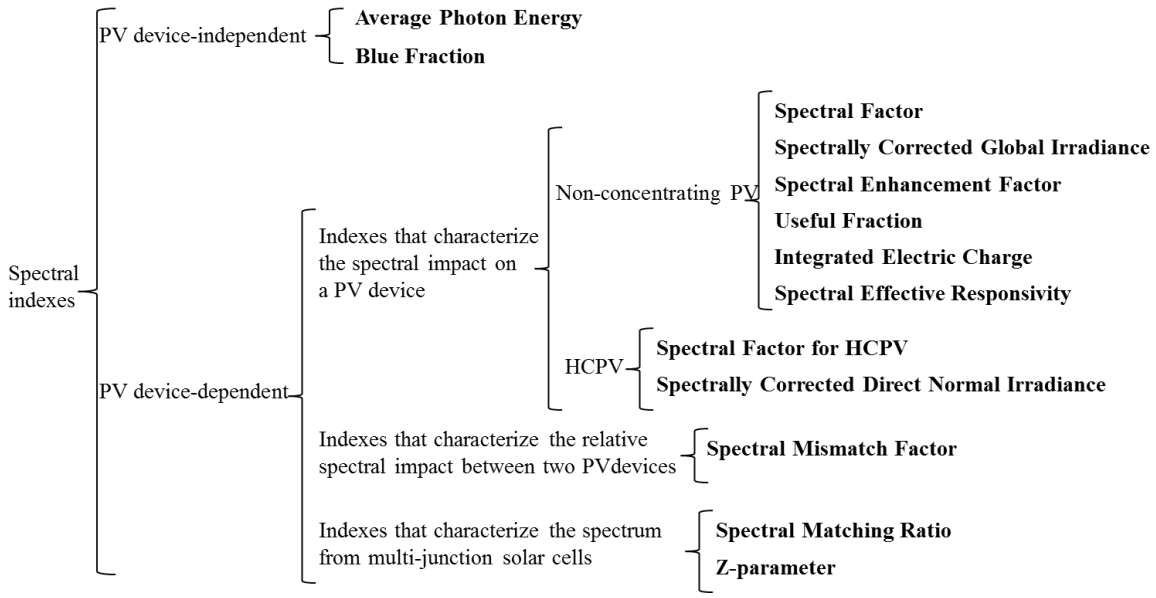

Fig. 4: Classification of indexes for quantifying spectral influences in photovoltaic systems.

3.1. PV device-independent indexes

3.1.1. Average Photon Energy

The "Average Photon Energy" index (APE) was first proposed by the Gottschalg's group of Loughborough University [29, 30] and has been used to characterize either the global spectrum or the direct spectrum in many works. APE is defined as the total irradiance contained in the spectrum divided by the total photon flux density. Relating to the global spectrum, its definition can be written as:

$$APE = \frac{\int_{\lambda_1}^{\lambda_2} E_G(\lambda) d\lambda}{q \int_{\lambda_1}^{\lambda_2} \Phi_G(\lambda) d\lambda} \quad (1)$$

$E_G(\lambda)$ being the actual global spectrum (W m^{-2} nm^{-1}) and $\Phi_G(\lambda)$ the photon flux density (photons m^{-2} s^{-1} nm^{-1}). q is a conversion factor ($1.6e^{-19}$ J/eV) equivalent to the electron charge. Thus, APE has units of electronVolts (eV). The photon flux density is calculated as:

$$\Phi_G(\lambda) = \frac{E_G(\lambda)}{hc/\lambda} \quad (2)$$

hc being the product of the Planck's constant by the light speed ($1.986e^{-16}$ J nm) and λ the wavelength (nm). The definition of APE for the direct spectrum is analogous to this but substituting the global spectrum $E_G(\lambda)$ by the direct spectrum $E_B(\lambda)$.

In Eq. (1), it is important to remark that APE is defined between two wavelength integration limits (λ_1 and λ_2). This means that, for the same spectrum, there are different APE values as a function of the defined integration limits. For instance, for the standard global spectrum, APE in the range 350-1050 nm is 1.88 eV, while APE in the range 300-1600 nm is 1.59 eV.

The meaning of the APE index is related to the sunlight chromatic distribution. By combining Eqs. (1) and (2), it can be seen that the spectrum $E_G(\lambda)$ in the denominator is multiplied by the wavelength, what means that low wavelength photons have less weight on the total photon flux density than high wavelength photons. So, as the chromatic distribution of the spectrum moves toward the infra-red wavelength range, the denominator in Eq. (1) increases and thus, the APE value decreases. Therefore, high APE values correspond to "blue-rich" spectra while low APE values correspond to "red-rich" spectra.

As can be seen from the definition of APE, this index is PV device-independent and only depends on the chromatic characteristics of the light (and, of course, on the defined wavelength integration limits, which are arbitrarily defined by the different authors).

Minemoto et al. [31] hypothesized the uniqueness between APE and spectrum. For this purpose, they analysed spectral measurements carried out at Kusatsu-city, Shiga-prefecture, Japan, by a statistical

procedure. This was based on selecting a lot of global spectra around a single APE value, dividing the wavelengths range into 50 nm intervals, calculating the energy percentages contained in each interval with respect to the overall spectrum energy and analysing the mean and standard deviation of the population. For every analysed wavelength interval, the standard deviation was lower than 0.39%. Authors concluded that the spectra that lead to the same APE value are virtually identical (at least for the site at which the measurements were made). This conclusion has been recently reinforced through spectral measurements carried out at JRC and NREL institutes, which also showed very low standard deviations [32]. However, the uniqueness APE-spectrum has been questioned by other authors. Gueymard [33] showed by means of simulations with the SMARTS spectral software that different direct spectra can lead to the same APE value, i.e. he found different combinations of air mass, aerosol optical depth and precipitable water that caused the same APE. This can be considered a theoretical proof against the uniqueness APE-spectrum at least for the direct sunlight spectrum. Later, Dirnberger et al. [17] carried out a detailed analysis of spectral measurements at Freiburg im Breisgau, Germany. They compared for many global spectra the APE value to the spectral losses on several PV modules. From the comparison, it was evident that a same APE value can generate different spectral losses in a PV device, what implies that different spectra can lead to the same APE. As a conclusion, these authors do not recommend APE as a good indicator for quantifying instantaneous spectral gains or losses. Similar conclusions can be found in other studies [34, 35]. Anyhow, APE has been widely used for the instantaneous spectral analysis in the literature what indicates that it is a practical index useful for qualitative analysis at least.

From the instantaneous APE, another index can be derived that relates to the spectral gains or losses in terms of energy, i.e. over a period of time. This index has been named as “Weighted Average APE” (<APE>) and is defined for the global spectrum as:

$$\langle APE \rangle = \frac{\sum_i G_i \cdot APE_i}{\sum_i G_i} \tag{3}$$

Namely, this energetic index is obtained by weighting the instantaneous APE_i values with the broadband irradiance G_i over a period of time. This way, <APE>· is more influenced by the APE_i values that take place for the highest irradiance values, at which the energy production of a PV module is higher. In contrast with the instantaneous APE index, <APE> has been recognized as a good indicator for the analysis of spectral energy gains or losses over a period of time, although it has been remarked that other PV device-dependent indexes can provide superior accuracy [17, 34].

The “Weighted Average APE” can be defined in the same way for the direct sunlight spectrum by substituting the global irradiance G_i by the direct normal irradiance B_i.

There is not a direct relation between APE (or <APE>) and the spectral gains or losses of a PV device. This relation must be indirectly found through regression or similar analysis and there are many works which have tried this analysis for different PV technologies, both for non-concentrating technologies [11, 10, 9, 36, 37, 38, 39, 40, 41, 42] [43] and for HCPV technologies [44, 45]. As an example of this kind of analysis, Fig. 5 shows a plot which represents the Performance Ratio (PR) of an m-Si PV and of an HCPV module as a function of APE.

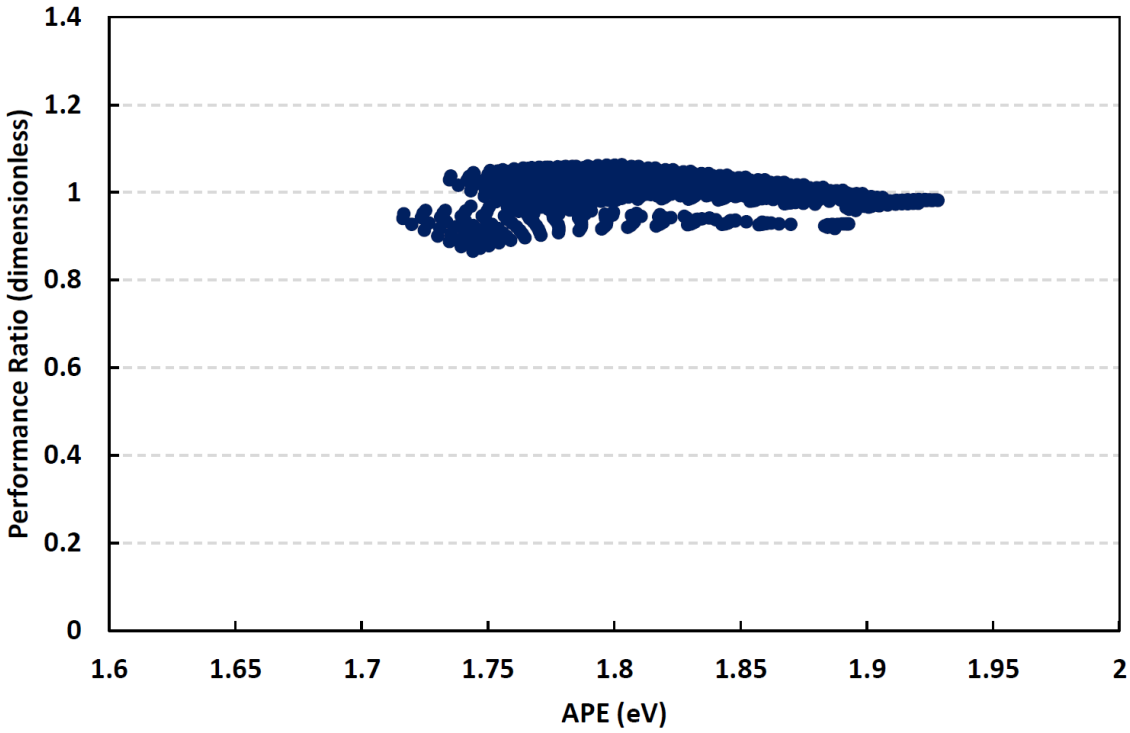
Performance Ratio (dimensionless)
1.4
1.2
1
0.8
0.6
0.4
0.2
0
1.6
1.65
1.7
1.75
1.8
1.85
1.9
1.95
2
APE (eV)

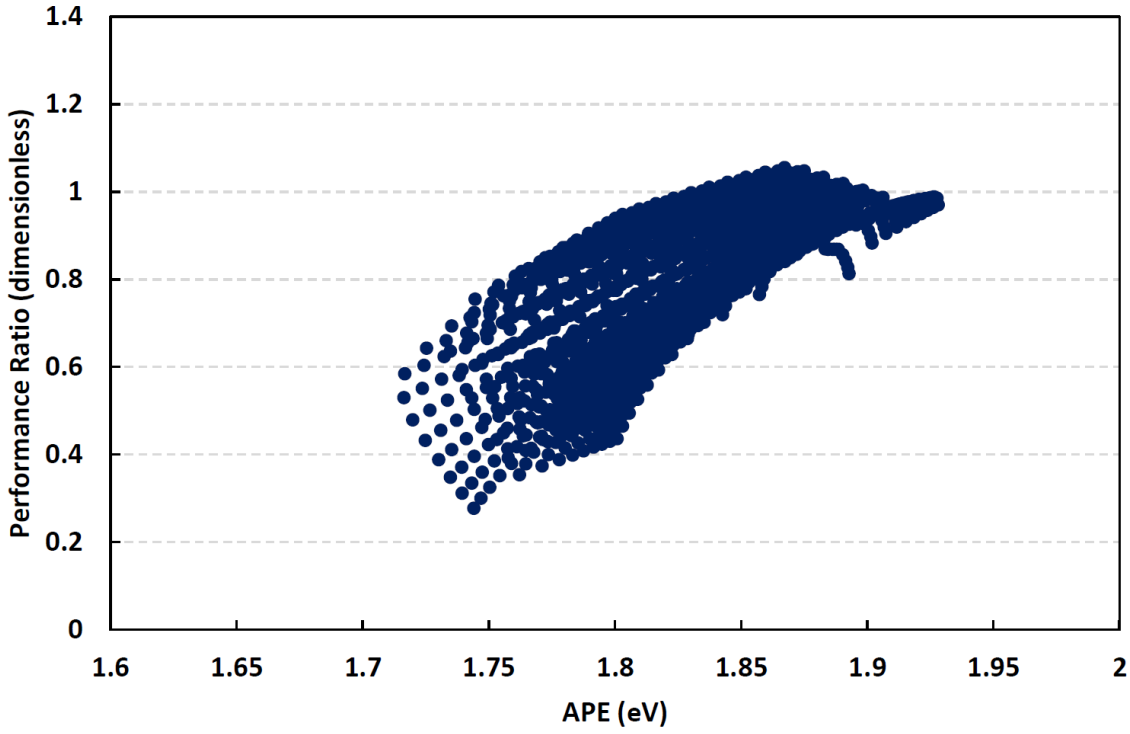
Performance Ratio (dimensionless)
1.4
1.2
1
0.8
0.6
0.4
0.2
0
1.6
1.65
1.7
1.75
1.8
1.85
1.9
1.95
2
APE (eV)

Fig. 5: Performance Ratio (PR) as a function of APE for a m-Si PV (top) and for an HCPV module made up of LM triple-junction solar cells and PMMA Fresnel lenses (bottom) recorded during March 2016 by a solar spectral irradiance meter (SolarSIM-D2) at the Centre for Advanced Studies in Energy and Environment at the University of Jaen, Spain. The integration limits of the APE are in the range 350-1050 nm. The spectral Performance Ratio in the y-axis represents the quotient between the maximum power of the device only accounting for irradiance and spectral effects and the ideal maximum power only accounting for irradiance effects.

The main advantage of these indexes is that they are PV device-independent, i.e. they can be used ignoring physical characteristics of the PV modules under study. On the other hand, they have the inherent disadvantages of the use of spectroradiometers, which are expensive, difficult to calibrate and require continuous maintenance and regular calibration. Also, the relation with the spectral gains or losses of a PV device is not easy to get and can be somewhat imprecise.

Kataoka et al. [46] proposed another index which tries to characterize the spectrum from the integrated irradiance of two spectral bands: a low wavelength band (450-500 nm) and a high wavelength band (800-850 nm). The aim was avoiding the use of a spectroradiometer and replacing it by two pyranometers with bandpass filters. This "multi-band APE" was defined as:

$$APE_{band} = \frac{\int_{450}^{500} E_G(\lambda)d\lambda + \int_{800}^{850} E_G(\lambda)d\lambda}{q\left(\frac{\int_{450}^{500} E_G(\lambda)d\lambda}{hc/475} + \frac{\int_{800}^{850} E_G(\lambda)d\lambda}{hc/825}\right)} \quad (4)$$

Authors reported an analysis of the uniqueness between APE_{band} and spectrum and concluded that this is a reasonably good index for characterizing the spectrum if a spectroradiometer is not available.

3.1.2. Blue Fraction

Another index for characterizing the blueness of the spectrum is the "Blue Fraction" [47]. In this method, the blue portion of the spectrum is considered to include the wavelengths below 650 nm. The "Blue Fraction" for the global spectrum is defined as:

$$BF = \frac{\int_{\lambda<650} E_G(\lambda)d\lambda}{\int E_G(\lambda)d\lambda} \quad (5)$$

i.e. this index represents the fraction of the broadband irradiance which is included inside the defined "blue band". It is an adimensional index. The higher the BF, the higher the energetic content of the blue portion of the spectrum as in the case of APE. For the standard global spectrum and integrating the irradiance until 1050 nm, BF has a value of 0.52. This means that BF values above 0.52 correspond to spectra with more blue content than the standard spectrum and vice versa. The index is PV device-independent but has similar disadvantages than the APE index: the need of a spectroradiometer and the vagueness of the relation between the index and the spectral gains or losses of a photovoltaic device.

3.2. PV device-dependent indexes

3.2.1. Indexes that characterize the spectral impact on a PV device

3.2.1.1. Non-concentrating PV devices

3.2.1.1.1. Spectral Factor

The "Spectral Factor" (SF) of a non-concentrating PV device is defined as:

$$SF = \frac{\int E_G(\lambda) SR(\lambda) d\lambda}{\int E_G^*(\lambda) SR(\lambda) d\lambda} \cdot \frac{\int E_G^*(\lambda) d\lambda}{\int E_G(\lambda) d\lambda} \quad (6)$$

$E_G^*(\lambda)$ being the reference global spectrum (W m^{-2} nm^{-1}) and $SR(\lambda)$ the spectral response of the device (A/W) at the reference cell temperature (usually 25ºC of cell temperature). It is an adimensional index. Fig. 1-top shows typical spectral response functions used in the calculation of the spectral factor for five kinds of PV materials.

SF corresponds with the "Spectral Mismatch Factor" (MM) of the IEC 60904-7 standard [48] (as will be reviewed later) by setting as reference PV device an ideal device with flat spectral response over the whole wavelengths range of solar radiation. This reference device can be implemented in practice with a pyranometer, operating under a thermoelectric principle rather than a photoelectric principle.

The SF index can be alternatively expressed as:

$$SF = \frac{I_{sc}}{I_{sc}^*} \cdot \frac{G^*}{G} \quad (7)$$

Where I_{sc} represents the short-circuit current of the PV device only accounting for irradiance and spectral effects, G the broadband irradiance (as measured by a plane-of-array pyranometer), I_{sc}^* the short-circuit current of the device at reference conditions and G^* the reference broadband irradiance corresponding to the standard spectrum $E_G^*(\lambda)$.

This instantaneous index is directly related to the spectral power gains or losses of the PV device. The electrical power is measured at the maximum power point of the device I-V curve while the SF index refers to the short-circuit current. However, it is well-known that in most solar cells the maximum power changes in the same proportion than the short-circuit current (only taking into account irradiance and spectral effects) [49, 50] and therefore, it can be written:

$$\frac{I_{sc}}{I_{sc}^*} \approx \frac{P_{\max}}{P_{\max}^*} \quad (8)$$

Thus, by substituting into Eq. (7), the following is obtained:

$$SF = \frac{P_{\max}}{P_{\max}^* \left(G/G^*\right)} \quad (9)$$

As can be seen, this expression takes the classical form of an instantaneous PV Performance Ratio. Numerator represents the maximum power of the PV device only accounting for irradiance and spectral effects, while denominator represents the maximum power only accounting for irradiance effects. Thus, the quotient represents the spectral power gains (if greater than 1) or losses (if lower than 1) in the PV device with respect to the reference spectrum. The Spectral Factor equals 1 when the incident spectrum equals the reference spectrum.

Eqs. (6) and (7) provide two alternative ways of measuring the SF. On the one hand, SF can be measured by means of a spectroradiometer with upper wavelength range greater than the limit wavelength at which the absorption takes place in the analysed PV material, Eq. (6). This alternative has the advantage that the SF is directly calculated and needs no corrections. However, the spectral response of the material must be known and this information is not always available (or it must be measured with a specific SR characterization set-up). Also, the drawbacks of using a spectroradiometer have already been mentioned. On the other hand, SF can be measured by monitoring the short-circuit current of the PV device under analysis, Eq. (7), without the need of a spectroradiometer and without knowing the spectral response function. The disadvantage of this procedure is that the measured short-circuit current must be corrected to remove temperature effects and, even more difficult, to remove angle-of-incidence effects. Finding accurate methods to perform these corrections is not always possible. So, both alternatives have pros and cons.

The SF as defined above has been used as a method to quantify instantaneous spectral gains or losses in several works [17, 43, 16, 13, 12, 28]. Also, Nann and Emery [51] used a "spectral efficiency ratio" (η/η^*) understood as the quotient between the efficiency only accounting for spectral effects and the reference efficiency. As efficiency is the ratio of the electrical power (P_{max}) to the incident luminous power ($G \cdot A$, A being the solar cell area), the following can be written:

$$\frac{\eta}{\eta^*} = \frac{P_{max}/(G \cdot A)}{P^*_{max}/(G^* \cdot A)} = \frac{P_{max}}{P^*_{max}(G/G^*)} = SF \tag{10}$$

i.e. the spectral efficiency ratio is equivalent to the SF.

Other authors used the "Inverse Spectral Factor" (SF^{-1}) [34, 42, 7, 8]. This index has the opposite meaning than the Spectral Factor: it takes values greater than 1 to represent spectral losses with respect to the reference spectrum and values lower than 1 to represent spectral gains. Finally, it has been used a "Relative Spectral Factor" (ΔSF) [13, 12, 28] or "Spectral Weighted Factor" (SWF) [35] defined as:

$$\Delta SF = SWF = SF - 1 \tag{11}$$

Which expresses the spectral gains (positive value) or losses (negative value) in per unit. As can be seen, SF, SF^{-1}, η/η^*, ΔSF or SWF have similar meanings and definitions.

As in the case of APE, an energetic index can be derived from the instantaneous SF, which is named "Weighted Average Spectral Factor" (<SF>). This is defined as:

$$\langle SF \rangle = \frac{\sum_i G_i \cdot SF_i}{\sum_i G_i} \tag{12}$$

This index is directly related to the spectral gains or losses with respect to the reference spectrum in terms of energy. Indeed, by applying the definition of the instantaneous SF one gets:

$$\langle SF \rangle = \frac{\sum_i G_i \cdot \frac{\int E_{Gi}(\lambda) SR(\lambda) d\lambda}{\int E_G^*(\lambda) SR(\lambda) d\lambda} \cdot \frac{G^*}{G_i}}{\sum_i G_i} \tag{13}$$

Which can be rearranged as:

$$\langle SF \rangle = \frac{\sum_i \int E_{Gi}(\lambda) SR(\lambda) d\lambda}{\int E_G^*(\lambda) SR(\lambda) d\lambda} \cdot \frac{G^*}{\sum_i G_i} \tag{14}$$

Or, in terms of the short-circuit currents:

$$\langle SF \rangle = \frac{\sum_i I_{sci}}{I_{sc}^*} \cdot \frac{G^*}{\sum_i G_i} \tag{15}$$

Taking into account that the quotient I_{sci}/I_{sc}^* can be approximated by P_{maxi}/P_{max}^* as explained above, the expression becomes:

$$\langle SF \rangle = \frac{\sum_i P_{\max i}}{P_{\max}^*} \cdot \frac{G^*}{\sum_i G_i} = \frac{\sum_i P_{\max i}}{\sum_i P_{\max}^* \left(G_i / G^* \right)} \tag{16}$$

And finally, multiplying and dividing by the time interval at which the measurements are made (Δt):

$$\langle SF \rangle = \frac{\sum_i P_{\max i} \cdot \Delta t}{\sum_i P_{\max}^* \left(G_i / G^* \right) \cdot \Delta t} \tag{17}$$

Numerator of this expression is the energy generated over the period of time only accounting for irradiance and spectral effects, while denominator is the energy generated only accounting for irradiance effects. Thus, <SF> expresses the energy spectral gains (if greater than 1) or losses (if lower than 1) over the period of time with respect to the reference spectrum. Fig. 6 shows an example of simulated monthly weighted average spectral factor values for different PV technologies at Jaén, Spain.

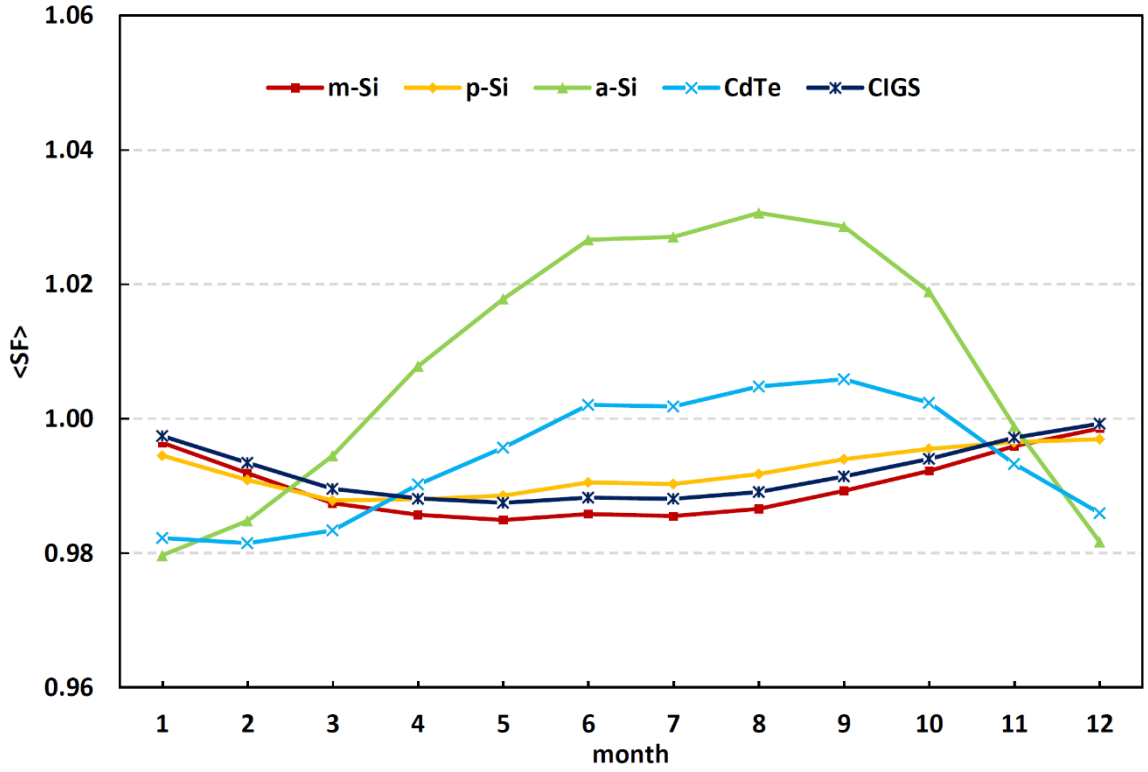

Fig. 6: Simulated monthly weighted average spectral factor values for different PV technologies at Jaen, Spain, following the procedure described in [28]. m-Si: mono-crystalline silicon; p-Si: poly-crystalline silicon; a-Si: amorphous silicon; CdTe: cadmium telluride; CIGS: copper indium gallium selenide The seasonal variation of the energy spectral gains or losses can be appreciated in the graph, especially for a-Si and CdTe technologies.

The main advantage of the SF and related indexes is that, if properly measured, they provide a direct and accurate quantification of the spectral gains or losses of a PV device. However, there are some drawbacks. As was commented, the calculation of these indexes requires both a spectroradiometer and knowledge of the spectral response function, or alternatively correcting the monitored short-circuit current in temperature and angle-of-incidence, what implies difficulties to obtain the indexes. Also, over a period of time, extensive computation is required to solve the convolution integral $\int E_{Gi}(\lambda)SR(\lambda)d\lambda$ at each time step.

3.2.1.1.2. Spectrally Corrected Global Irradiance

The "Spectrally Corrected Global Irradiance" or "Spectrally Effective Global Irradiance" (G_c) can be defined as:

$$G_c = \frac{\int E_G(\lambda)SR(\lambda)d\lambda}{\int E_G^*(\lambda)SR(\lambda)d\lambda} \cdot \int E_G^*(\lambda)d\lambda \qquad (18)$$

In units of W/m^2. This instantaneous index expresses the irradiance effectively available for the photovoltaic conversion taking into account the spectral response of the analysed photovoltaic device. The index is closely related to the Spectral Factor, i.e. the following direct relation is verified:

$$SF = \frac{G_c}{G} \tag{19}$$

Thus, the spectral power gains or losses of a photovoltaic device can be calculated by the ratio of the Spectrally Corrected Global Irradiance and the broadband irradiance. This concept has been used in several works [17, 34, 43]. As in the case of the Spectral Factor, it can be measured by means of a spectroradiometer, Eq. (18), or alternatively through the short-circuit current as:

$$G_c = \frac{I_{sc}}{I_{sc}^*} \cdot G^* \tag{20}$$

With the same difficulties commented in the previous section.

A related energetic index which could be named as "Spectrally Corrected Global Irradiation" (H_c) can be calculated by integrating G_c over a period of time:

$$H_c = \sum_i G_{ci} \cdot \Delta t \tag{21}$$

In units of Wh/m^2. This index represents the irradiation effectively available for the photovoltaic conversion over a period of time. It's easy to prove that the following relation with the Weighted Averaged Spectral Factor verifies:

$$\langle SF \rangle = \frac{H_c}{H} \tag{22}$$

H being the global irradiation incident on the PV device over the analysed interval. Thus, H_c can also be used to quantify spectral energy gains or losses with respect to the reference spectrum over a period of time.

3.2.1.1.3. Spectral Enhancement Factor

An energetic index has been used, with variants, to quantify spectral energy gains or losses over a period of time, which slightly differs from the <SF>. Here, we name it "Spectral Enhancement Factor" (SEF) according to the nomenclature in [33]. It is defined as:

$$SEF = \frac{\int \langle E_G(\lambda) \rangle SR(\lambda) d\lambda}{\int E_G^*(\lambda) SR(\lambda) d\lambda} \cdot \frac{\int E_G^*(\lambda) d\lambda}{\overline{G}} \tag{23}$$

In this expression, $<E_G(\lambda)>$ is the "Average Incident Spectrum" [33], also named "Weighted Solar Spectrum" (WSS) [52], and represents the average solar spectrum weighted by the irradiance over the period of time:

$$\langle E_G(\lambda)\rangle = \frac{\sum_i G_i \cdot E_{Gi}(\lambda)}{\sum_i G_i} \tag{24}$$

On the other hand, $\overline{G}$ is the mean irradiance over the period of time:

$$\overline{G} = \frac{\sum_i G_i}{N} \tag{25}$$

N being the number of measurements taken at constant time intervals.

When comparing this index to the <SF>, an advantage looks evident: the convolution integral is solved once for the Average Incident Spectrum, instead of solving it at each time step for the instantaneous spectrum as is required in the <SF> index. However, in order to get this easier calculation, the index assumes the following approach:

$$\frac{\int \langle E_G(\lambda)\rangle SR(\lambda)d\lambda}{\overline{G}} \approx \frac{\sum_i \int E_{Gi}(\lambda)SR(\lambda)d\lambda}{\sum_i G_i} \tag{26}$$

Which can be also written as:

$$\int \langle E_G(\lambda)\rangle SR(\lambda)d\lambda \approx \frac{1}{N}\sum_i \int E_{Gi}(\lambda)SR(\lambda)d\lambda \tag{27}$$

That is, this index tries to approximate the <SF> under the assumption that the convolution integral of the Average Incident Spectrum approximately equals the mean of the convolution integrals of the instantaneous spectra. If this assumption is good, the meaning of the SEF index is analogous to that of the <SF> index: it represents the energy spectral gains (if greater than 1) or losses (if lower than 1) over the period of time with respect to the reference spectrum.

The “Inverse Spectral Enhancement Factor” (SEF^{-1}) has been also used in the literature [52, 53]. These authors simply named the index as “Spectral Factor”. The meaning of SEF^{-1} is energy spectral losses with respect to the reference spectrum for values greater than 1 and energy spectral gains for values lower than 1.

As was mentioned, the main advantage of SEF or SEF^{-1} with respect to <SF> is the ease of calculation. However, we could not find in the consulted works an analysis of the goodness of the assumption represented in Eq. (27).

3.2.1.1.4. Useful Fraction

The “Useful Fraction” instantaneous index (UF) was proposed in [54, 55] and can be defined as:

$$UF = \frac{\int_{\lambda<\lambda_0} E_G(\lambda)d\lambda}{\int E_G(\lambda)d\lambda} \tag{28}$$

Where λ_0 is the upper wavelength at which the absorption takes place in the photovoltaic material. This way, UF represents the fraction of the spectrum power available for the photovoltaic conversion. The index is PV device-dependent because different semiconductor materials have different absorption limits λ_0. It is an adimensional index. Fig. 7 graphically shows the absorption bands of four PV materials in comparison to the standard global spectrum.

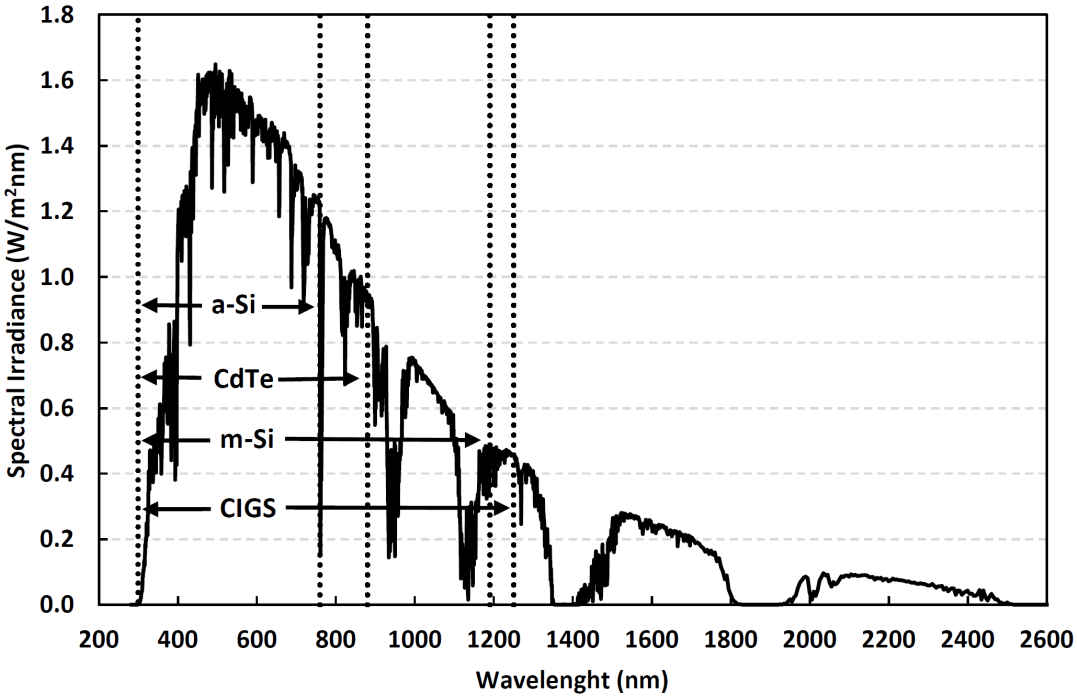

Fig. 7: Standard AM 1.5 global spectrum and corresponding absorption band of four PV materials: m-Si: mono-crystalline silicon; a-Si: amorphous silicon; CdTe: cadmium telluride; CIGS: copper indium gallium selenide.

UF can represent spectral power gains or losses through its relation to the "Reference Useful Fraction" (UF^*). This UF^* is the Useful Fraction under the reference spectrum:

$$UF^* = \frac{\int_{\lambda<\lambda_0} E_G^*(\lambda)d\lambda}{\int E_G^*(\lambda)d\lambda} \tag{29}$$

The ratio between both magnitudes can be named "Useful Fraction Ratio" (UF/UF^*) [56]:

$$\frac{UF}{UF^*} = \frac{\int_{\lambda<\lambda_0} E_G(\lambda)d\lambda}{\int_{\lambda<\lambda_0} E_G^*(\lambda)d\lambda} \cdot \frac{\int E_G^*(\lambda)d\lambda}{\int E_G(\lambda)d\lambda} \tag{30}$$

When comparing this expression with the definition of the SF index, Eq. (6), it can be seen that the Useful Fraction Ratio is equivalent to the Spectral Factor under the assumption that the material has

flat spectral response in the wavelength range at which the absorption takes place, and zero spectral response outside this range. That is, the Useful Fraction Ratio is a way of approximating the Spectral Factor by assuming ideal absorption properties of the photovoltaic material. Thus, the meaning of the UF/UF* index is spectral gains with respect to the reference spectrum (if greater than 1) or spectral losses (if lower than 1) by assuming an idealized photovoltaic material.

The corresponding energetic index of UF is the "Integrated Useful Fraction" (IUF), which indicates the percentage of the incident energy over a period of time that is available for the photovoltaic conversion:

$$IUF = \frac{\sum_i \int_{\lambda<\lambda_0} E_{Gi}(\lambda) d\lambda}{\sum_i \int E_{Gi}(\lambda) d\lambda} \tag{31}$$

The ratio between this magnitude and the "Reference Integrated Useful Fraction" (IUF*) can be named "Integrated Useful Fraction Ratio" (IUF/IUF*), which has at the end the following definition:

$$\frac{IUF}{IUF^*} = \frac{\sum_i \int_{\lambda<\lambda_0} E_{Gi}(\lambda) d\lambda}{\int_{\lambda<\lambda_0} E_G^*(\lambda) d\lambda} \cdot \frac{G^*}{\sum_i G_i} \tag{32}$$

When comparing this expression with Eq. (14), it can be seen that the Integrated Useful Fraction Ratio is equivalent to the Weighted Average Spectral Factor, except that it has been assumed flat spectral response in the wavelengths range at which the absorption takes place in the photovoltaic material, and zero spectral response outside this range.

The main advantage of these indexes is that knowledge of the spectral response function is not required (they only need the limit wavelength at which the absorption takes place in the photovoltaic material), so they are useful if this function is not available. However, a comparison between the Useful Fraction and an accurate index such as the Spectral Factor has not yet been reported to be able to quantify the error induced by the idealized properties of the material.

3.2.1.1.5. Integrated Electric Charge

The energetic index named "Integrated Electric Charge" (Q) was introduced in [57] understood as the integral of the device short-circuit current density only accounting for irradiance and spectral effects over a period of time:

$$Q = \sum_i \int E_{Gi}(\lambda) SR(\lambda) d\lambda \cdot \Delta t \tag{33}$$

It has units of Ah/m^2 or, more conveniently, Ah/cm^2. This index gives information about the spectral energy gains or losses by comparison to the "Reference Integrated Electric Charge" (Q*), that is the Integrated Electric Charge calculated considering the reference spectrum:

$$Q^* = \sum_i \int E_G^*(\lambda) SR(\lambda) d\lambda \cdot \Delta t = N \cdot \int E_G^*(\lambda) SR(\lambda) d\lambda \cdot \Delta t \tag{34}$$

It is easy to prove that the "Integrated Electric Charge Ratio" (Q/Q^*) verifies the following relation with the Weighted Average Spectral Factor (<SF>):

$$\langle SF \rangle = \frac{Q}{Q^*} \cdot \frac{G^*}{\overline{G}} \tag{35}$$

i.e. the energy spectral gains or losses with respect to the reference spectrum can be calculated from the Q/Q^* index if pyranometer measurements of G_i are available over the period of analysis.

The advantage of these indexes is that they do not require themselves the use of a reference pyranometer to be calculated (they can be exclusively calculated from spectroradiometer measurements). However, if one wants to relate the index value with the energy spectral gains or losses with respect to the reference spectrum, the use of an additional pyranometer is mandatory, as can be seen in Eq. (35).

3.2.1.1.6. Spectral Effective Responsivity

The instantaneous index "Spectral Effective Responsivity" (S_{ef}) was defined in [58] as:

$$S_{ef} = \frac{\int E_G(\lambda) SR(\lambda) d\lambda}{\int_{\lambda<\lambda_0} E_G(\lambda) d\lambda} \tag{36}$$

λ_0 being the upper wavelength at which the absorption takes place in the photovoltaic material. The index expresses in units of A/W the ratio between the short-circuit current only accounting for irradiance and spectral effects and the spectrum power available for the photovoltaic conversion.

This index is related to the Spectral Factor and the Useful Fraction by means of:

$$SF = S_{ef} \cdot UF \cdot \frac{G^*}{\int E_G^*(\lambda) SR(\lambda) d\lambda} \tag{37}$$

As in the previously reviewed index, this index itself has the advantage that it can be exclusively calculated through spectroradiometer measurements without the need of a pyranometer. However, if one wants to relate the index value to the spectral gains or losses with respect to the reference spectrum, the use of a pyranometer is mandatory to obtain the UF in Eq. (37).

3.2.1.2. HCPV devices

3.2.1.2.1. Spectral Factor for HCPV

HCPV modules are more complex than non-concentrating PV modules because they incorporate in assembly optical elements and multi-junction solar cells, in addition to some other peripheral elements. Thus, the behaviour of these modules is influenced by effects which are not present in non-concentrating PV devices. This implies that the measurement or calculation of spectral gains or losses in these modules is more difficult than in non-concentrating devices.

Although the concept of Spectral Factor for HCPV is under development, it has been reported a Spectral Factor index (SF_{HCPV}) which incorporates the main spectral effects influencing HCPV modules [28, 15, 59]. This index was defined as:

$$SF_{HCPV} = \frac{\min_j \left\{ \int E_B(\lambda) \eta_{opt}(\lambda) SR_j(\lambda) d\lambda \right\}}{\min_j \left\{ \int E_B^*(\lambda) \eta_{opt}(\lambda) SR_j(\lambda) d\lambda \right\}} \cdot \frac{\int E_B^*(\lambda) d\lambda}{\int E_B(\lambda) d\lambda} \quad (38)$$

$E_B(\lambda)$ and $E_B^*(\lambda)$ being respectively the actual and reference direct spectra, $\eta_{opt}(\lambda)$ the spectral optical efficiency of the HCPV module and $SR_j(\lambda)$ the spectral response of the j-th junction in the multi-junction solar cell at the reference cell temperature. As can be seen, the index takes into account the current-matching effect in multi-junction solar cells (the short-circuit current of a two-terminal multi-junction cell is limited by the subcell with lower short-circuit current) by selecting the minimum of the convolutions integrals of the different junctions. Also, the index approximates the incident spectrum on the solar cell by the product of the external direct spectrum $E_B(\lambda)$ by the spectral optical efficiency of the HCPV module $\eta_{opt}(\lambda)$. This way, two important characteristics of HCPV devices spectral behaviour are accounted for by the index: the current-matching and the change in the spectral content of the light when overpassing the optical elements.

Obviously, the authors have idealized the behaviour of an HCPV module in several ways when defining this index: the spectral optical efficiency of the HCPV module has been kept time-invariant, while it is known that the optical properties of the lenses change as a function mainly of the lens temperature (which varies with the atmospheric conditions) [60]; and it has been assumed no chromatic aberrations due to the optical elements which could cause a non-uniform incident spectrum on the solar cell surface [61]. In spite of these idealizations, the index seems to be a valuable approximation to the instantaneous spectral gains or losses of a realistic HCPV module.

According to Eq. (38), the SF_{HCPV} index could be measured with the help of a spectroradiometer with collimator tube and a reference pyrheliometer. The SF_{HCPV} index calculation requires knowledge of the spectral responses of the subcells at the reference cell temperature and the spectral optical efficiency of the HCPV module at a representative lens temperature.

The same authors proposed another version of this index as [62]:

$$SF_{HCPV} = \frac{I_{sc}^{meas}}{I_{sc}^*} \cdot \frac{B^*}{B} \quad (39)$$

I_{sc}^{meas} being the actual short-circuit current measured on the HCPV device, I_{sc}^* the reference short-circuit current, B the actual direct normal irradiance and B^* the reference direct normal irradiance. This version has also been named as "Normalized I_{sc}" in [63]. It avoids the use of a spectroradiometer by monitoring the short-circuit current and it has the advantage that every optical effect in the HCPV device is accounted for, as the real response of the solar cell is measured through its short-circuit current. However, there are some drawbacks: the short-circuit current is not measured at the reference cell temperature but at changing temperature as a function of the atmospheric conditions [64]; and also, the non-ideal motion of the sun tracker can create certain noise in the measured short-circuit currents [65].

As can be seen, these indexes approximate the spectral gains or losses with respect to the reference spectrum as in the case of the Spectral Factor for non-concentrating PV devices, i.e. index values greater than 1 mean spectral gains and index values lower than 1 mean spectral losses. Authors have also used the "Relative Spectral Factor" (ΔSF_{HCPV}) defined as in the case of non-concentrating devices as $\Delta SF_{HCPV}=SF_{HCPV}-1$. It takes positive values for spectral gains and negative values for spectral losses.

Also, Muller et al. [66] used the "Change in the I_{sc}/DNI ratio" understood as the change in the I_{sc}/DNI ratio with respect to the I_{sc}/DNI ratio at reference conditions normalized to the I_{sc}/DNI ratio at reference conditions. It can be written as:

$$Change\, I_{sc}/DNI = \frac{I_{sc}/B - I_{sc}^{*}/B^{*}}{I_{sc}^{*}/B^{*}} = \frac{I_{sc}}{I_{sc}^{*}} \cdot \frac{B^{*}}{B} - 1 = SF_{HCPV} - 1 = \Delta SF_{HCPV} \tag{40}$$

i.e. the "Change in the I_{sc}/DNI ratio" is equivalent to the "Relative Spectral Factor".

Of course, as in the case of non-concentrating PV devices, the "Weighted Average Spectral Factor for HCPV" ($<SF_{HCPV}>$) has been used to quantify spectral energy gains or losses over a period of time as [28, 15]:

$$\left\langle SF_{HCPV} \right\rangle = \frac{\sum_i B_i \cdot SF_{HCPVi}}{\sum_i B_i} \tag{41}$$

Fig. 8 shows an example of simulated monthly weighted average spectral factor values for four different structures of HCPV modules at Jaén, Spain.

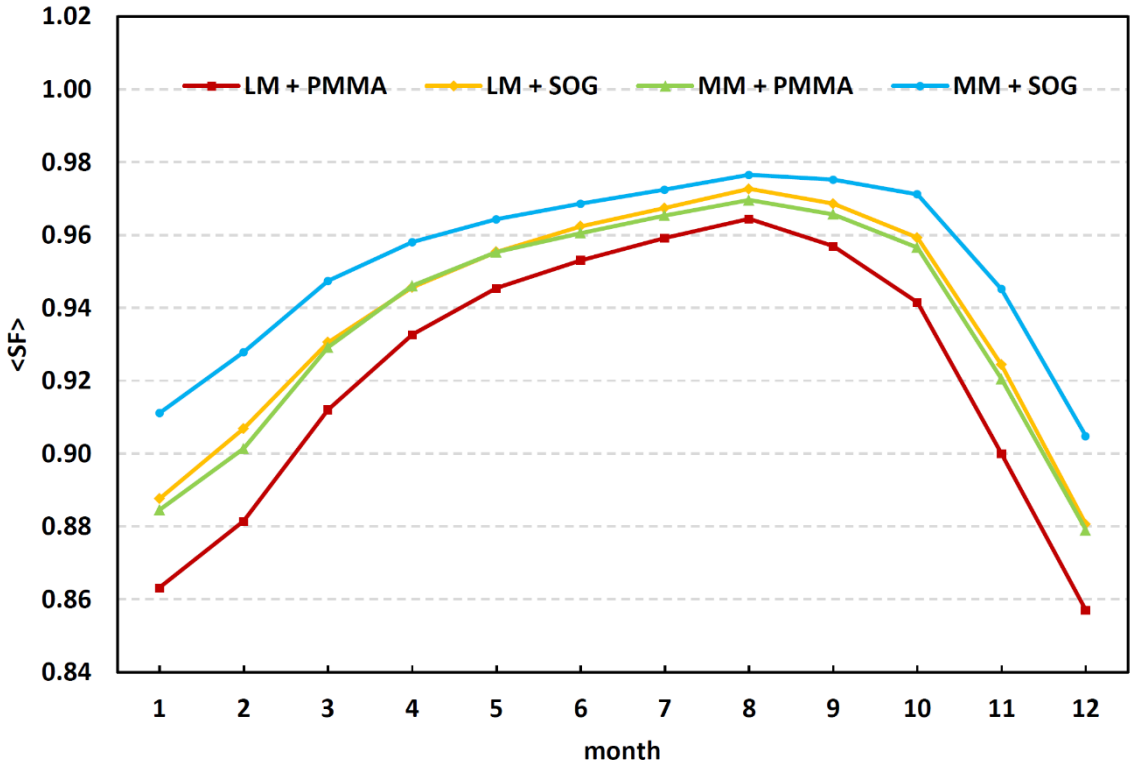

Fig. 8: Simulated monthly weighted average spectral factor values for different structures of HCPV modules at Jaen, Spain, following the procedure described in [28]. LM: GaInP/GaInAs/Ge lattice-matched solar cell; MM: GaInP/GaInAs/Ge metamorphic solar cell; PMMA: poly(methyl methacrylate) Fresnel lens; SOG: silicon-on-glass Fresnel lens. The seasonal variation of the energy spectral gains or losses can be appreciated in the graph for all the HCPV modules.

3.2.1.2.2. Spectrally Corrected Direct Normal Irradiance

The concept of "Spectrally Corrected Direct Normal Irradiance" (B_c) in HCPV is similar to that in non-concentrating PV but applied to the direct normal radiation, i.e. it tries to express the direct irradiance effectively available for the photovoltaic conversion taking into account the spectral response of the analysed photovoltaic device. Nowadays, there are two research lines related to this index: on the one hand, some authors are linking this concept to the "Spectral Factor for HCPV"; on the other hand, some authors are trying to measure the B_c through the use of component cells.

The first research line defines the "Spectrally Corrected Direct Normal Irradiance" from the SF_{HCPV} as reviewed in the previous section [15]:

$$B_c = \frac{\min_j \left\{ \int E_B(\lambda)\eta_{opt}(\lambda)SR_j(\lambda)d\lambda \right\}}{\min_j \left\{ \int E_B^*(\lambda)\eta_{opt}(\lambda)SR_j(\lambda)d\lambda \right\}} \cdot \int E_B^*(\lambda)d\lambda \quad (42)$$

or alternatively as [67, 68]:

$$B_c = \frac{I_{sc}^{meas}}{I_{sc}^*} \cdot B^* \tag{43}$$

This Spectrally Corrected Direct Normal Irradiance is directly related to the Spectral Factor for HCPV by:

$$SF_{HCPV} = \frac{B_c}{B} \tag{44}$$

i.e. it is useful to quantify realistic spectral gains or losses on the HCPV device under the mentioned idealizations of its behaviour or assuming a small noise in the measurements as was commented.

The second research line is based on the use of component cells. A component cell is equivalent to a multi-junction solar cell in which only one of the subcells is electrically connected. An instrument composed of as many component cells as the number of junctions of the analysed multi-junction solar cell is named as spectroheliometer. The spectroheliometer provides an easier and cheaper way of performing spectral measurements than a spectroradiometer. This instrument provides the short-circuit current of each component cell, which is supposed to be similar to the photocurrent of the corresponding junction of the multi-junction solar cell under the condition that each component cell has identical or almost equal spectral response than the corresponding junction in the multi-junction device.

For a spectroheliometer composed of N_{MJ} component cells, it can be defined N_{MJ} Spectrally Corrected Direct Normal Irradiances (B_{c1}, B_{c2}, …, B_{cNmj}) as [69]:

$$B_{cj} = \frac{I_{scj}^{c.c.}}{I_{scj}^*} \cdot B^*, \quad j = 1,2,...,N_{NJ} \tag{45}$$

$I_{scj}^{c.c.}$ being the actual short-circuit current measured on the j-th component cell, I_{scj}^* the reference short-circuit current of the j-th component cell and B^* the reference direct normal irradiance. Now, let us name I_{sc}^* as the minimum of the reference short-circuit currents of the component cells:

$$I_{sc}^* = \min_j \left\{ I_{scj}^* \right\} \tag{46}$$

The Spectrally Corrected Direct Normal Irradiance as measured by the spectroheliometer is defined as [70]:

$$B_c = \min_j \left\{ B_{cj} \cdot \frac{I_{scj}^*}{I_{sc}^*} \right\} \tag{47}$$

An equivalent expression for B_c can be obtained by substituting B_{cj} by its value in Eq. (45):

$$B_c = \min_j \left\{ \frac{I_{scj}^{c.c.}}{I_{sc}^*} \cdot B^* \right\} = \frac{\min_j \left\{ I_{scj}^{c.c.} \right\}}{I_{sc}^*} \cdot B^* = \frac{\min_j \left\{ I_{scj}^{c.c.} \right\}}{\min_j \left\{ I_{scj}^* \right\}} \cdot \int E_B^*(\lambda) d\lambda \tag{48}$$

The last expression can be compared to the definition of the Spectrally Corrected Direct Normal Irradiance linked to the Spectral Factor for HCPV in Eq. (42). The conclusion is that both approaches are very similar. The approach based on component cells tries to approximate the short-circuit current of the HCPV device by the short-circuit current as measured by the component cells.

Thus, both approaches are very similar from an analytical point of view. However, from a practical point of view, there are important differences. The approach that links the B_c to the Spectral Factor for HCPV tries to represent realistic spectral gains or losses on an HCPV module. However, the approach based on component cells is a farther approximation which goes after a practical measurement of the spectrum, rather than after an accurate calculation of spectral gains or losses. There are three main reasons because the component cells are only able to approximate the spectral gains or losses of a real HCPV module: first, the component cells operate under non-concentrated sunlight, i.e. they cannot capture the influences of the optical elements that are present in a real HCPV module; second, the component cells do not operate at the reference cell temperature (as it would be required to avoid thermal effects on the short-circuit current), but at changing temperature as a function of the atmospheric conditions; third, it would not be possible to have as many spectroheliometers as kinds of multijunction solar cells, so in many cases, the absorption band of the component cells is not identical than that of the multi-junction solar cells in the analysed HCPV module, but they have only similar spectral responses. In spite of these limitations, component cells seem to be a useful tool and have been proposed for the power rating of HCPV modules [69, 70, 71] or for improving the design of these modules by adapting to the spectral characteristics of a particular location [72]. Fig. 9 shows values of Spectrally Corrected Direct Normal Irradiances as measured by component cells for a lattice-matched triple junction solar cell during a summer day at Jaen, Spain, and compares to the Direct Normal Irradiance as measured by a pyrheliometer.

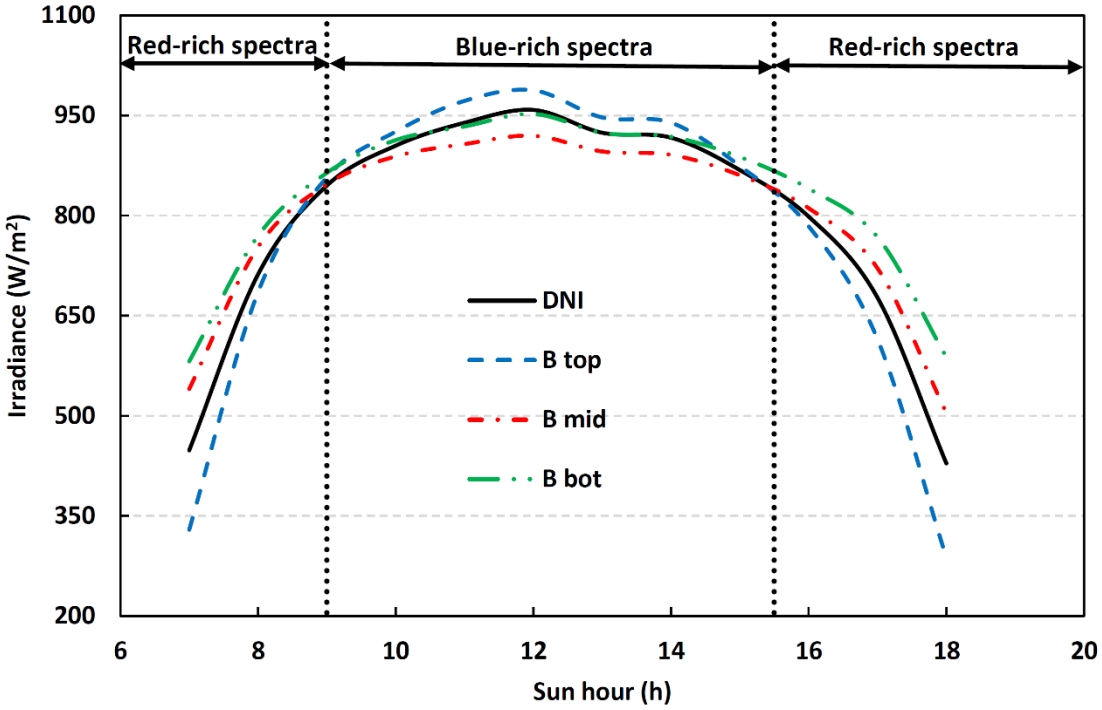

Fig. 9: Component cell measurements of Spectrally Corrected Direct Normal Irradiances (B_{top}, B_{mid}, B_{bot}) corresponding to a GaInP/GaInAs/Ge lattice-matched solar cell during 05/15/2016 at Jaén, Spain, and simultaneous measurements of Direct Normal Irradiance (DNI) by means of a pyrheliometer. As can be seen, at sunrise and sunset the top subcell limits the current because of red-rich spectra, while at the central hours of the day (the period at which most of the energy is generated) the middle cell limits the current because of blue-rich spectra. The operating points with a spectral status equivalent to the standard AM1.5d spectrum are indicated in the graph in dashed lines.

3.2.2. Indexes that characterize the relative spectral impact between two PV devices

3.2.2.1. Spectral mismatch factor

The "Spectral Mismatch Factor" (MM) is defined in the IEC 60904-7 standard [48] as a way of quantifying the relative spectral impact between a sample PV device and a reference PV device by means of:

$$MM_{sample/ref} = \frac{\int E_G(\lambda) SR_{sample}(\lambda) d\lambda}{\int E_G^*(\lambda) SR_{sample}(\lambda) d\lambda} \cdot \frac{\int E_G^*(\lambda) SR_{ref}(\lambda) d\lambda}{\int E_G(\lambda) SR_{ref}(\lambda) d\lambda} \quad (49)$$

Where $SR_{sample}(\lambda)$ represents the spectral response of the sample PV device and $SR_{ref}(\lambda)$ the spectral response of the reference PV device, both at the reference cell temperature. As can be seen from this definition, $MM_{sample/ref}$ accounts for spectral gains (if greater than 1) or spectral losses (if lower than 1) of the sample PV device with respect to the reference PV device. The index equals 1 when the incident spectrum equals the reference spectrum or when the two devices are spectrally matched, i.e. they have identical spectral responses.

The index can be measured with the help of a spectroradiometer if both the spectral response of the sample device and the spectral response of the reference device are known. However, there is an alternative based on the measurement of the short-circuit currents of both devices by means of the expression:

$$MM_{sample/ref} = \frac{I_{sc,sample}}{I_{sc,sample}^*} \cdot \frac{I_{sc,ref}^*}{I_{sc,ref}} \quad (50)$$

$I_{sc,sample}$ and $I_{sc,ref}$ being respectively the short-circuit currents of the sample device and the reference device only accounting for irradiance and spectral effects, $I_{sc,sample}^*$ and $I_{sc,ref}^*$ being respectively the reference short-circuit currents of the sample device and the reference device. Therefore, if the index is calculated through measurement of the short-circuit currents, they should be corrected in temperature and angle-of-incidence, or it must be assumed the corresponding error in the index value.

It is easy to prove that the Spectral Mismatch Factor can be seen as the ratio between the Spectral Factor of the sample PV device and the Spectral Factor of the reference PV device:

$$MM_{sample/ref} = \frac{SF_{sample}}{SF_{ref}} \quad (51)$$

Because of this, the $MM_{sample/ref}$ has also been named as "Spectral Factor of sample PV device relative to reference PV device" ($SF_{sample}/_{ref}$) as in [16].

3.2.3. Indexes that characterize the spectrum from multi-junction solar cells

3.2.3.1. Spectral Matching Ratio

The "Spectral Matching Ratio" (SMR) index has a similar definition than the Spectral Mismatch Factor (MM, as reviewed in the previous section). The difference is that, while the MM is applied to represent the relative spectral impact between a sample PV device and a reference PV device, the SMR is applied to two subcells in a multi-junction solar cell. This index is calculated through the measurements of component cells and can be defined as [70]:

$$SMR_{j/k} = \frac{I_{scj}^{c.c.}}{I_{scj}^{*}} \cdot \frac{I_{sck}^{*}}{I_{sck}^{c.c.}} \tag{52}$$

$I_{scj}^{c.c.}$ and $I_{sck}^{c.c.}$ being respectively the measured short-circuit currents on the j-th component cell and on the k-th component cell, I_{scj}^{*} and I_{sck}^{*} being respectively the reference short-circuit currents of the j-th component cell and of the k-th component cell. Thus, under the hypothesis that the j-th and the k-th subcells could operate independently, $SMR_{j/k}$ would represent the relative spectral impact on the j-th component cell with respect to the k-th component cell, having values greater than 1 for spectral gains of the j-th component cell with respect to the k-th component cell, or lower than 1 for spectral losses of the j-th component cell with respect to the k-th component cell. However, this hypothesis does not verify in practice, where the different subcells are series-connected in a multi-junction stack and subject to current-matching limitations. So, the index cannot be directly related to real spectral gains or losses in a multi-junction solar cell, and therefore, is only intended to assess the input direct spectral distribution.

$SMR_{j/k}$ can also be seen as the ratio of the Spectrally Corrected Direct Normal Irradiance of the j-th component cell (B_{cj}) to the Spectrally Corrected Direct Normal Irradiance of the k-th component cell (B_{ck}):

$$SMR_{j/k} = \frac{B_{cj}}{B_{ck}} \tag{53}$$

The "weighted average SMR" has been used in [73] to represent the relative spectral impact over a period of time as:

$$\left\langle SMR_{j/k} \right\rangle = \frac{\sum_i B_i SMR_{j/k,i}}{\sum_i B_i} \tag{54}$$

Nowadays, most HCPV modules are composed of triple-junction solar cells. In the commercial HCPV modules based on triple-junction solar cells operating in real conditions, the subcell which limits the device current can be either the top subcell or the middle subcell depending on the spectrum

of the incident light. This means that the most important SMR index that defines the spectral status of these triple-junction devices is the $SMR_{top/middle}$, which represents the spectral mismatch between the two possible limiting subcells: top and middle. The $SMR_{top/middle}$ as measured by component cells is defined as:

$$SMR_{top/middle} = \frac{I_{scTOP}^{c.c.}}{I_{scTOP}^{*}} \cdot \frac{I_{scMID}^{*}}{I_{scMID}^{c.c.}} = \frac{B_{cTOP}}{B_{cMID}} \tag{55}$$

Under the reference spectrum, the $SMR_{top/middle}$ equals 1. Normally, the reference spectrum is the AM1.5d ASTM G-173-03 [5] at which the multi-junction solar cells are rated and optimized, i.e.multi-junction solar cells are usually designed to provide the same short-circuit current of the top and middle subcells under the AM1.5d standard spectrum. If this is the case, under the AM1.5d standard spectrum, $SMR_{top/middle}$ equals 1and the short-circuit currents of the top and middle subcells are the same. With incident spectra with "more blue content" than the standard spectrum, the $SMR_{top/middle}$ is greater than 1 and the middle subcell limits the current, while with incident spectra with "more red content" than the standard spectrum, the $SMR_{top/middle}$ is lower than 1 and the top subcell limits the current. This way, the value of $SMR_{top/middle}$ indicates which subcell limits the current and how big is the difference between the photocurrents of both subcells. Of course, this discussion is only valid if the multi-junction solar cell verifies the mentioned design criterion [74].

As the information provided by the $SMR_{top/middle}$ index is very important to know the spectral status of a multi-junction solar cell, different authors have tried to correlate the $SMR_{top/middle}$ index as measured by component cells to electrical parameters of real HCPV modules operating in the field [45, 75]. This relation is not direct and requires regression or similar procedures because of the limitations of the spectroheliometers mentioned in the previous section, i.e. their behaviour necessarily differ from the behaviour of the real HCPV devices. Fig. 10 presents an example of the Spectral Factor of an HCPV module obtained from measurements of its short-circuit as a function of the $SMR_{top/middle}$ as measured by component cells.

The SMR index has been mainly evaluated in the literature from the measurements of component cells. Because of this, in this section, we have focused on defining this index from the short-circuit currents of component cells. However, it is remarkable that this index can be also evaluated from spectroradiometer measurements, by making use of the spectral response of a given multi-junction solar cell. The corresponding formulae can be easily derived from Eq. (52) and are not included here for brevity.

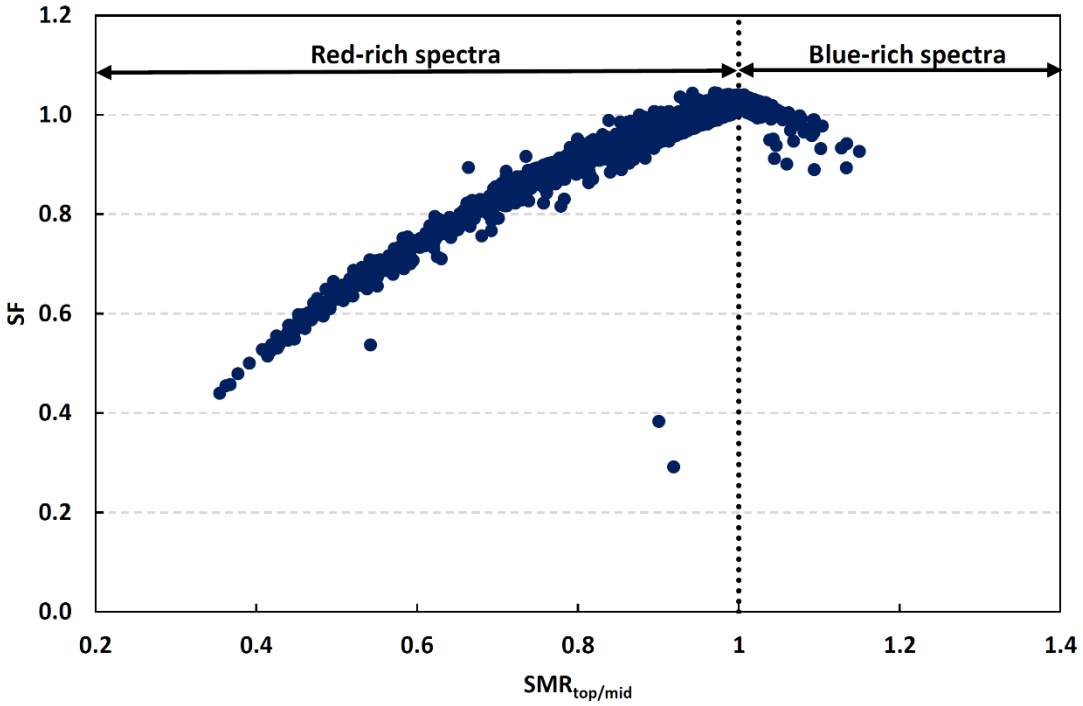

Fig. 10: Spectral Factor of an HCPV module made up of LM triple-junction solar cells and SOG Fresnel lenses calculated from measurements of its short-circuit current to the Spectral Matching Ratio (SMR) of the top subcell with respect to the middle subcell as measured during March 2016 by component cells at the Centre for Advanced Studies in Energy and Environment at the University of Jaen, Spain.

3.2.3.2. Z-parameter

The "Z-parameter" (Z) was first proposed in [76] as an index to assess the direct solar spectrum taking as inputs the short-circuit currents as measured by component cells. While it has been theoretically introduced for any kind of multi-junction solar cell, in practice it has been applied to commercial triple-junction III-V cells. The following explanation focuses on the Z-parameter for these kinds of cells.

The current ratios R_{TOP} and R_{MID} are defined as the ratio between the short-circuit current of the corresponding subcell as measured by a component cell and the reference short-circuit current of that subcell:

$$R_{TOP} = \frac{I_{scTOP}^{c.c.}}{I_{scTOP}^{*}}; \quad R_{MID} = \frac{I_{scMID}^{c.c.}}{I_{scMID}^{*}} \tag{56}$$

These ratios can be plotted in a two-dimensional plane known as the spectrometric plane, Fig. 11. In the spectrometric plane, a point represents a particular pair (R_{TOP},R_{MID}). A line R_{TOP}/R_{MID}=constant is a line through the origin; every point on this line has the same relative spectral balance between the

top and middle subcells ($SMR_{top/middle}$=constant). On the other hand, the line $R_{TOP}+R_{MID}=2$ is known as the spectrometric line.

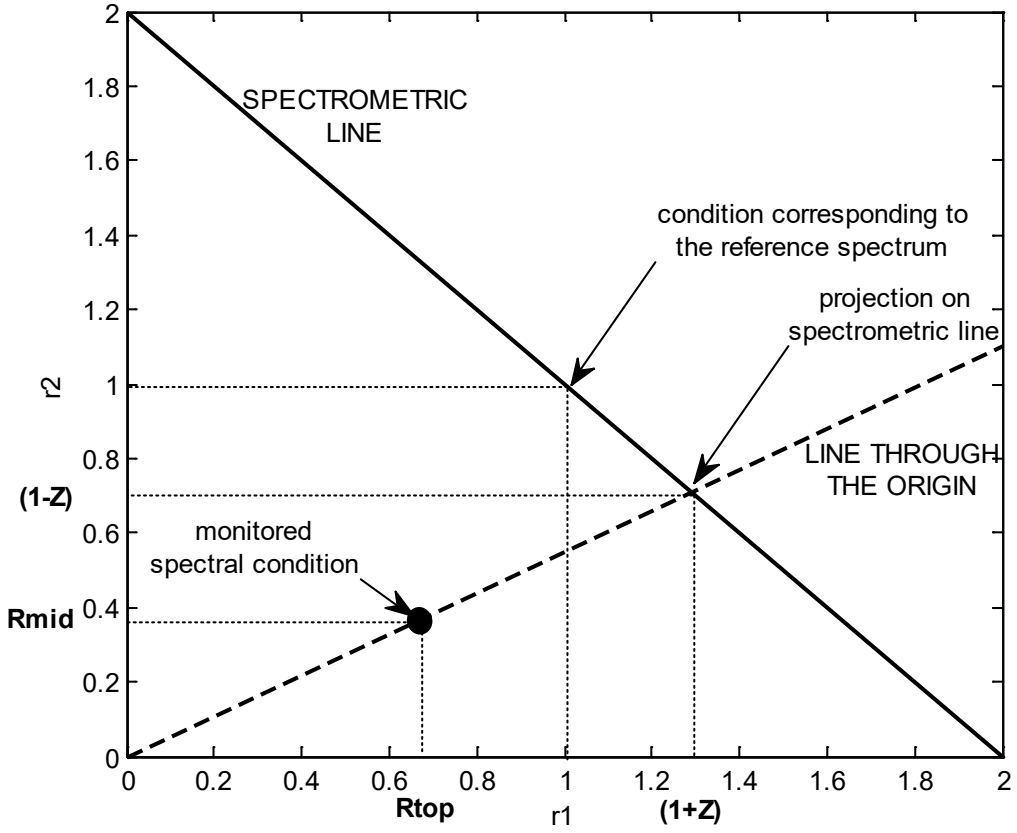

Fig. 11: Example of spectrometric plane used to define the Z-parameter. The x-axis corresponds to R_{TOP} and the y-axis corresponds to R_{MID}. The spectrometric line links the points (0,2) and (2,0). The point (1,1) on the spectrometric line corresponds to the reference spectrum condition. A monitored spectral condition (R_{TOP}, R_{MID}) is shown as a generic point on the spectrometric plane. This point is projected onto the spectrometric line by a line through the origin in order to define the Z-parameter for this spectral condition.

The Z-parameter for a pair (R_{TOP},R_{MID}) located on the spectrometric line is defined as:

$$Z(\textit{espectrometric line}) = 1 - R_{MID} = R_{TOP} - 1 \tag{57}$$

For a pair (R_{TOP},R_{MID}) not on the spectrometric line, the point can be projected by a line through the origin onto the spectrometric line, as seen in Fig. 11. The coordinates of the projected point (R_{TOP}',R_{MID}') can be expressed as:

$$R'_{TOP} = \frac{2 \cdot R_{TOP}}{R_{TOP} + R_{MID}}; \quad R'_{MID} = \frac{2 \cdot R_{MID}}{R_{TOP} + R_{MID}} \tag{58}$$

And thus, for a generic (R_{TOP},R_{MID}) point, the Z-parameter is defined as:

$$Z = 1 - R'_{MID} = R'_{TOP} - 1 \tag{59}$$

Which is equivalent to:

$$Z = \frac{R_{TOP} - R_{MID}}{R_{TOP} + R_{MID}} \tag{60}$$

This Z-parameter can be also expressed as a direct function of the $SMR_{top/middle}$. The $SMR_{top/middle}$ verifies:

$$SMR_{top\,/\,middle} = \frac{R_{TOP}}{R_{MID}} \tag{61}$$

And therefore, from Eq. (59),the following is obtained:

$$Z = \frac{SMR_{top\,/\,middle} - 1}{SMR_{top\,/\,middle} + 1} \tag{62}$$

As can be seen, the Z-parameter and the Spectral Matching Ratio are closely related. Under the hypothesis that the multi-junction solar cell is designed to provide the same short-circuit current of the top and middle subcells under the AM1.5d standard spectrum, Z=0 is equivalent to $SMR_{top/middle}=1$, and represents conditions at which the top and middle subcells generate the same current; Z>0 is equivalent to $SMR_{top/middle}>1$, and represents conditions at which the middle subcell limits the current; Z<0 is equivalent to $SMR_{top/middle}<1$, and represents conditions at which the top subcell limits the current.

As in the case of the $SMR_{top/middle}$ index, authors have tried to correlate the Z-parameter with the behaviour of real HCPV modules in spite of the commented limitations of the component cells for these purposes [71, 76]. Fig. 12 presents an example of the Spectral Factor of an HCPV module obtained from measurements of its short-circuit current as a function of the Z-parameter as measured by component cells.

Finally, it is remarkable that, while the Z-parameter has been evaluated in the literature from the measurement of component cells, and this is the approach discussed in this section, it could be also evaluated from spectroradiometer measurements by making use of the spectral response of a given multi-junction solar cell, as in the case of the SMR index.

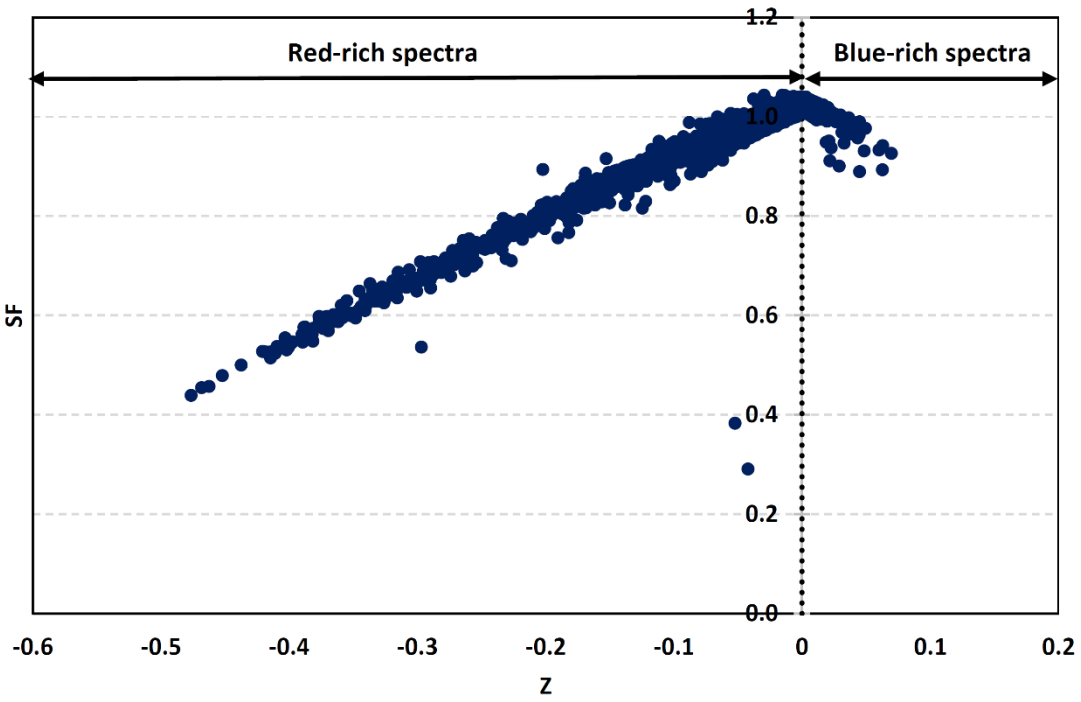

Fig. 12: Spectral Factor of an HCPV module made up of LM triple-junction solar cells and SOG Fresnel lenses calculated from measurements of its short-circuit current to the Z-parameter of the top subcell with respect to the middle subcell as measured during March 2016 by component cells at the Centre for Advanced Studies in Energy and Environment at the University of Jaen, Spain.

After completing the review of spectral indexes, two comparative tables are presented. Table 2 synthetizes the main advantages and disadvantages of the reviewed indexes. Table 3 summarizes the definitions of the indexes and their type (instantaneous or energetic). These comparative tables can be useful for understanding the relations between the available spectral indexes and for selecting the most suitable index for each specific application.

Table 2
Advantages and disadvantages of the spectral indexes used in the literature

Index	**Advantages**	**Disadvantages**
Average Photon Energy / Blue Fraction	PV device-independent	It requires spectroradiometer Relation with spectral gains or losses is not direct Moderate accuracy because it does not consider the PV device
Spectral Factor / Spectrally Corrected Global Irradiance	Direct and accurate calculation of spectral gains or losses It can be measured through the short-circuit current	It requires spectroradiometer and knowledge of the spectral response, or alternatively: It requires correcting the monitored short-circuit current Extensive computation for energy calculation
Spectral Enhancement Factor	Ease of calculation	It requires spectroradiometer and knowledge of the spectral response Degree of accuracy not reported
Useful Fraction	Spectral response not required Ease of calculation	It requires spectroradiometer Degree of accuracy not reported
Integrated Electric Charge	The index itself does not require pyranometer	It requires spectroradiometer and knowledge of the spectral response, or alternatively: It requires correcting the monitored short-circuit current Extensive computation for energy calculation Pyranometer required to relate to the spectral gains or losses
Spectral Effective Responsivity	The index itself does not require pyranometer	It requires spectroradiometer and knowledge of the spectral response Extensive computation for energy calculation Pyranometer required to relate to the spectral gains or losses
Spectral Factor for HCPV / Spectrally Corrected Direct	Direct and accurate calculation of spectral gains or losses It can be measured through the short-circuit current	It requires spectroradiometer and knowledge of the spectral response and spectral optical efficiency, or alternatively:

Normal Irradiance (linked to the Spectral Factor)		There is noise in the monitored short-circuit current Extensive computation for energy calculation
Spectrally Corrected Direct Normal Irradiance (through component cells)	It requires spectroheliometer instead of spectroradiometer Ease of calculation	Relation with spectral gains or losses is not direct Moderate accuracy due to the limitations of the component cells
Spectral Mismatch Factor	Direct and accurate calculation of spectral gains or losses It can be measured through the short-circuit current	It requires spectroradiometer and knowledge of the spectral response, or alternatively: It requires correcting the monitored short-circuit current Extensive computation for energy calculation
Spectral Matching Ratio / Z-parameter	It requires spectroheliometer instead of spectroradiometer Ease of calculation	Relation with spectral gains or losses is not direct Moderate accuracy due to the limitations of the component cells

Table 3
Definition of the spectral indexes used in the literature and type

Index	**Symbol / Units**	**Type**	**Definition**
Average Photon Energy	APE eV	Instantaneous	$\frac{\int_{\lambda_1}^{\lambda_2} E(\lambda)d\lambda}{(q/hc)\int_{\lambda_1}^{\lambda_2} \lambda \cdot E(\lambda)d\lambda}$; $E(\lambda)=E_G(\lambda)$ (*global spectrum*) $E(\lambda)=E_B(\lambda)$ (*direct spectrum*)
Weighted Average APE	<APE> eV	Energetic	$\sum_i \frac{\int E_i(\lambda)d\lambda \cdot \int_{\lambda_1}^{\lambda_2} E_i(\lambda)d\lambda}{(q/hc)\int_{\lambda_1}^{\lambda_2} \lambda \cdot E_i(\lambda)d\lambda}$; $\frac{}{\sum_i \int E_i(\lambda)d\lambda}$ $E_i(\lambda)=E_{Gi}(\lambda)$ (*global spectrum*) $E_i(\lambda)=E_{Bi}(\lambda)$ (*direct spectrum*)
Blue Fraction	BF adim.	Instantaneous	$\frac{\int_{\lambda<650} E_G(\lambda)d\lambda}{\int E_G(\lambda)d\lambda}$
Spectral Factor	SF adim.	Instantaneous	$\frac{\int E_G(\lambda)SR(\lambda)d\lambda}{\int E_G^*(\lambda)SR(\lambda)d\lambda} \cdot \frac{\int E_G^*(\lambda)d\lambda}{\int E_G(\lambda)d\lambda}$
Inverse Spectral Factor	SF^{-1} adim.	Instantaneous	$\frac{\int E_G^*(\lambda)SR(\lambda)d\lambda}{\int E_G(\lambda)SR(\lambda)d\lambda} \cdot \frac{\int E_G(\lambda)d\lambda}{\int E_G^*(\lambda)d\lambda}$
Relative Spectral Factor	ΔSF adim.	Instantaneous	$\frac{\int E_G(\lambda)SR(\lambda)d\lambda}{\int E_G^*(\lambda)SR(\lambda)d\lambda} \cdot \frac{\int E_G^*(\lambda)d\lambda}{\int E_G(\lambda)d\lambda} - 1$
Weighted Average Spectral Factor	<SF> adim.	Energetic	$\frac{\sum_i \int E_{Gi}(\lambda)SR(\lambda)d\lambda}{\int E_G^*(\lambda)SR(\lambda)d\lambda} \cdot \frac{\int E_G^*(\lambda)d\lambda}{\sum_i \int E_{Gi}(\lambda)d\lambda}$
Spectrally Corrected Global Irradiance	G_c W/m^2	Instantaneous	$\frac{\int E_G(\lambda)SR(\lambda)d\lambda}{\int E_G^*(\lambda)SR(\lambda)d\lambda} \cdot \int E_G^*(\lambda)d\lambda$
Spectrally Corrected Global Irradiation	H_c Wh/m^2	Energetic	$\frac{\int E_G^*(\lambda)d\lambda}{\int E_G^*(\lambda)SR(\lambda)d\lambda} \cdot \sum_i \int E_{Gi}(\lambda)SR(\lambda)d\lambda \cdot \Delta t$
Spectral Enhancement Factor	SEF adim.	Energetic	$\frac{\int \left(\frac{\sum_i \int E_{Gi}(\lambda)d\lambda \cdot E_{Gi}(\lambda)}{\sum_i \int E_{Gi}(\lambda)d\lambda} \right) SR(\lambda)d\lambda}{\int E_G^*(\lambda)SR(\lambda)d\lambda} \cdot \frac{\int E_G^*(\lambda)d\lambda}{(1/N)\sum_i \int E_{Gi}(\lambda)d\lambda}$
Inverse Spectral Enhancement Factor	SEF^{-1} adim.	Energetic	$\frac{\int E_G^*(\lambda)SR(\lambda)d\lambda}{\int \left(\frac{\sum_i \int E_{Gi}(\lambda)d\lambda \cdot E_{Gi}(\lambda)}{\sum_i \int E_{Gi}(\lambda)d\lambda} \right) SR(\lambda)d\lambda} \cdot \frac{(1/N)\sum_i \int E_{Gi}(\lambda)d\lambda}{\int E_G^*(\lambda)d\lambda}$

Useful Fraction	UF adim.	Instantaneous	$\frac{\int_{\lambda<\lambda_0} E_G(\lambda)d\lambda}{\int E_G(\lambda)d\lambda}$
Useful Fraction Ratio	UF/UF* adim.	Instantaneous	$\frac{\int_{\lambda<\lambda_0} E_G(\lambda)d\lambda}{\int_{\lambda<\lambda_0} E_G^*(\lambda)d\lambda} \cdot \frac{\int E_G^*(\lambda)d\lambda}{\int E_G(\lambda)d\lambda}$
Integrated Useful Fraction	IUF adim.	Energetic	$\frac{\sum_i \int_{\lambda<\lambda_0} E_{Gi}(\lambda)d\lambda}{\sum_i \int E_{Gi}(\lambda)d\lambda}$
Integrated Useful Fraction Ratio	IUF/IUF* adim.	Energetic	$\frac{\sum_i \int_{\lambda<\lambda_0} E_{Gi}(\lambda)d\lambda}{\int_{\lambda<\lambda_0} E_G^*(\lambda)d\lambda} \cdot \frac{\int E_G^*(\lambda)d\lambda}{\sum_i \int E_{Gi}(\lambda)d\lambda}$
Integrated Electric Charge	Q Ah/m^2	Energetic	$\sum_i \int E_{Gi}(\lambda)SR(\lambda)d\lambda \cdot \Delta t$
Integrated Electric Charge Ratio	Q/Q* adim.	Energetic	$\frac{(1/N)\cdot \sum_i \int E_{Gi}(\lambda)SR(\lambda)d\lambda}{\int E_G^*(\lambda)SR(\lambda)d\lambda}$
Spectral Effective Responsivity	S_{ef} A/W	Instantaneous	$\frac{\int E_G(\lambda)SR(\lambda)d\lambda}{\int_{\lambda<\lambda_0} E_G(\lambda)d\lambda}$
Spectral Factor for HCPV	SF_{HCPV} adim.	Instantaneous	$\frac{\min_j \left\{\int E_B(\lambda)\eta_{opt}(\lambda)SR_j(\lambda)d\lambda\right\}}{\min_j \left\{\int E_B^*(\lambda)\eta_{opt}(\lambda)SR_j(\lambda)d\lambda\right\}} \cdot \frac{\int E_B^*(\lambda)d\lambda}{\int E_B(\lambda)d\lambda}$
Relative Spectral Factor for HCPV	ΔSF_{HCPV} adim.	Instantaneous	$\frac{\min_j \left\{\int E_B(\lambda)\eta_{opt}(\lambda)SR_j(\lambda)d\lambda\right\}}{\min_j \left\{\int E_B^*(\lambda)\eta_{opt}(\lambda)SR_j(\lambda)d\lambda\right\}} \cdot \frac{\int E_B^*(\lambda)d\lambda}{\int E_B(\lambda)d\lambda} - 1$
Weighted Average Spectral Factor for HCPV	$<SF_{HCPV}>$ adim.	Energetic	$\frac{\sum_i \min_j \left\{\int E_{Bi}(\lambda)\eta_{opt}(\lambda)SR_j(\lambda)d\lambda\right\}}{\min_j \left\{\int E_B^*(\lambda)\eta_{opt}(\lambda)SR_j(\lambda)d\lambda\right\}} \cdot \frac{\int E_B^*(\lambda)d\lambda}{\sum_i \int E_{Bi}(\lambda)d\lambda}$
Spectrally Corrected Direct Normal Irradiance	B_c W/m^2	Instantaneous	$\frac{\min_j \left\{\int E_B(\lambda)\eta_{opt}(\lambda)SR_j(\lambda)d\lambda\right\}}{\min_j \left\{\int E_B^*(\lambda)\eta_{opt}(\lambda)SR_j(\lambda)d\lambda\right\}} \cdot \int E_B^*(\lambda)d\lambda; \quad (linked\ to\ SF_{HCPV})$ $\frac{\min_j \left\{I_{scj}^{c.c.}\right\}}{\min_j \left\{I_{scj}^*\right\}} \cdot \int E_B^*(\lambda)d\lambda; \quad (component\ cells)$

Spectrally Corrected Direct Normal Irradiation	H_{Bc} Wh/m^2	Energetic	$\frac{\sum_i \min_j \left\{\int E_{Bi}(\lambda)\eta_{opt}(\lambda)SR_j(\lambda)d\lambda\right\}}{\min_j \left\{\int E_B^*(\lambda)\eta_{opt}(\lambda)SR_j(\lambda)d\lambda\right\}} \cdot \int E_B^*(\lambda)d\lambda \cdot \Delta t; \quad (linked\ to\ SF_{HCPV})$ $\frac{\sum_i \min_j \left\{I_{scij}^{c.c.}\right\}}{\min_j \left\{I_{scj}^*\right\}} \cdot \int E_B^*(\lambda)d\lambda \cdot \Delta t; \quad (component\ cells)$
Spectral Mismatch Factor	MM adim.	Instantaneous	$\frac{\int E_G(\lambda)SR_{sample}(\lambda)d\lambda}{\int E_G^*(\lambda)SR_{sample}(\lambda)d\lambda} \cdot \frac{\int E_G^*(\lambda)SR_{ref}(\lambda)d\lambda}{\int E_G(\lambda)SR_{ref}(\lambda)d\lambda}$
Spectral Matching Ratio	$SMR_{j/k}$ adim.	Instantaneous	$\frac{I_{scj}^{c.c.}}{I_{scj}^*} \cdot \frac{I_{sck}^*}{I_{sck}^{c.c.}}$
Weighted Average SMR	$<SMR_{j/k}>$ adim.	Energetic	$\frac{\sum_i \int E_{Bi}(\lambda)d\lambda \cdot \frac{I_{scj,i}^{c.c.}}{I_{scj}^*} \cdot \frac{I_{sck}^*}{I_{sck,i}^{c.c.}}}{\sum_i \int E_{Bi}(\lambda)d\lambda}$
Z-parameter	Z adim.	Instantaneous	$\frac{\frac{I_{scTOP}^{c.c.}}{I_{scTOP}^*} \cdot \frac{I_{scMID}^*}{I_{scMID}^{c.c.}} - 1}{\frac{I_{scTOP}^{c.c.}}{I_{scTOP}^*} \cdot \frac{I_{scMID}^*}{I_{scMID}^{c.c.}} + 1}$

4. Annual spectral energy gain or loss values in the literature

The annual energy harvesting could be considered as the most relevant magnitude for the analysis of the performance of photovoltaic systems and one of the most important parameters influencing their profitability [77, 78, 79]. At the same time, the accurate evaluation of the spectral effects has demonstrated to have a far from negligible impact on the energy yield and cost of electricity estimations of photovoltaic facilities [80, 25]. Bearing this in mind, this section aims to discuss the most relevant results concerning the spectral impact at annual time scale of non-concentrating and high-concentrating PV devices available in the literature, which are summarized in Tables 3 and 4. Detailed information of the methodology followed by each author can be found in the references provided in the tables. In any case, the full description of the calculations involved in the findings obtained by the different authors can be also found in the previous section. It is important to remark that the technologies listed virtually cover all the photovoltaic market share, and therefore, the results shown could be considered representative of the current photovoltaic technology.

The studies analysed have been grouped in two tables: a) Table 3 presents studies regarding non-concentrating PV technology, while b) Table 4 presents studies regarding HCPV technology. The tables cover the behaviour of both technologies over a wide range of worldwide locations with different latitudes and weather characteristics. So, the results allow the performance of the different photovoltaic systems to be studied and compared under disparate climatic conditions. In addition, the annual average values of the crucial weather variables for understanding the spectral behaviour of photovoltaic devices at each specific site (i.e. air mass, aerosol optical depth and precipitable water) have been included. The air mass has been estimated by using the Gueymard formulaprovided in Section 2 as a function of the Sun´s zenith angle calculated every 60 seconds. The rest of weather

variables at each location have been taken from the Aerosol Robotic Network (AERONET) database when a station was available. The AERONET program is a federation of ground-based sun photometer sensors established by NASA and PHOTONS which started in the early 1990s [81], and offers measurements of AOD and PW, and other relevant parameters at remote sites for three data quality levels (i.e. Level 1, Level 1.5 and Level 2). In this case, the highest quality assured data (Level 2) has been used. Based on the data provided in Tables 4 and 5, the two following main concerns can be addressed, namely, a) to contribute to the understanding of the spectral coupling of the atmosphere and the yield of photovoltaic devices depending on their absorption bands, and b) to help in the selection of the most appropriate photovoltaic technology depending on the required application at each particular site.

Table 4 shows the annual energy spectral impact for several PV materials with low (i.e. c-Si, CIGS and CIS) and high (a-Si and CdTe) energy gaps. The latitude of the locations ranges from a minimum of around 1.3º (Singapore) to a maximum of around 48.8º (Stuttgart). With regards to AOD, a minimum value of 0.07 is found in Frenchman Flat, since is a clay desert site characterized by a clear atmosphere, while an extreme maximum value of 0.7 is found in Beijing, due to the fact that is a highly polluted industrialized city. Regarding PW, a minimum value of 0.7 cm is found in Tamanrasset, dominated by a dry hot dessert climate, while an extreme maximum value of 4.52 cm is found in the tropical climate location of Singapore. As can be seen, the results are in agreement with the commented in Section 2. The materials with low energy gap show similar results and a noteworthy stable spectral performance. The energy spectral effects range from -1.7% (Beijing) to 1.5% (Sttutgart) for c-Si, from -1.2% (Frenchman Flat and Solar Village) to 1.8% (Sttutgart) for CIGS, and from -1.4% (Tamanrasset) to -0.6% (Sttutgart) for CIS. On the other hand, the materials with high energy gap show a remarkable spectral dependence. The energy spectral effects range from -7.8% (Beijing) to 8.8% (Okinoerabu) for a-Si, and from -4.5% (Beijing) to 3.0% (Singapore) for CdTe. The extremely different results obtained for these materials can be understood by considering the different climatic variables at each location and the sensitivity analysis conducted in Section 2. For instance, the high energy losses found in Beijing are due to the red-rich spectral distribution produced by the extreme values of AOD. On the contrary, the high energy gains obtained in Singapore are produced by the blue-rich spectral distribution caused by the low latitude (low AM values) and extreme PW values.

Table 5 shows the annual energy spectral impact for several HCPV systems made up of different multi-junction solar cells and primary optics (i.e. LM, LM + PMMA, LM + SOG, MM + PMMA and MM + SOG). In this case, the latitude of the locations ranges from a minimum of around -9.9º (Alta Floresta) to a maximum of around 40.4º (Madrid). The minimum and maximum values of AOD are found at the same locations previously commented for the PV materials. With regards to PW, in this case, a minimum value of 0.9 cm is found in the dry dessert location of Frenchman Flat, while an extreme maximum value of 3.9 cm is found in the tropical site of Alta Floresta. As expected, the performance of HCPV systems shows a higher spectral dependence than PV systems, and present important spectral losses for every location. Overall, these losses are mainly dominated by the limitation of the current of the top junction caused by its high energy gap, and range from approximately -30.6% (Beijing) for LM + PMMA to -3.9% (Alta Floresta) for LM + SOG. As for high energy gap PV materials, the spectral performance can be understood by analysing the characteristic weather variables at each location and the fundamental analysis conducted in Section

2. The extremely high spectral losses at Beijing are dominated by a systematic limitation of the current of the top junction of the assembly due to the notable red-rich spectral distribution produced by the high AOD values. On the contrary, the minimum spectral losses at Alta Floresta are produced by the blue-rich spectral distribution caused by the low latitude (low AM values) and extreme PW values. It is also important to remark that the system based on MM solar cells and SOG Fresnel lenses tends to have the best spectral performance. This can be explained by considering the red shift of the absorption bands of the top and middle junctions of MM solar cells and because the usual higher transmittance of SOG Fresnel lenses in the spectral region of the top junction.

Table 4
Estimated relative annual average spectral impact for different PV technologies in percentage.

Location	Latitude (º)	AM	AOD	PW (cm)	c-Si	a-Si	CdTe	CIGS	CIS	Reference
Sapporo (Japan)	43.05	3.82	-	-	0.2	1.3	-	-	-	[34]
Tosu[1] (Japan)	33.38	3.42	0.31	1.93	0.4	1.3	-	-	-	[34]
Gifu (Japan)	35.42	3.49	-	-	0.2	1.3	-	-	-	[34]
Okinoerabu (Japan)	27.37	3.25	-	-	0.2	8.8	-	-	-	[34]
Madrid (Spain)	40.39	3.69	0.10	1.25	-0.7 to -0.6	-1.0 to 1.4	-1.5 to 0.3	-	-0.9	[16]
Jaén[2] (Spain)	37.77	3.58	0.10	1.25	-0.7 to -0.5	0.0 to 2.0	-0.5 to 0.6	-	-1.0	[16]
Sttutgart[3] (Germany)	48.78	4.17	0.20	1.46	-0.6	-0.4	-0.5	-	-0.6	[16]
Sttutgart[3] (Germany)	48.78	4.17	0.20	1.46	1.5	2.5	2.1	1.8		[57]
Tamanrasset (Algeria)	22.78	3.15	0.23	0.74	-1.2 to -1.0	2.2	0.1		-1.4	[16]
Freiburg (Germany)	47.99	4.13	-	-	1.4	3.4	2.4	0.6	-	[17]
Singapore (Singapore)	1.29	2.95	0.37	4.52	-	7.0	3.0	0.0	-	[82]
Solar Village (Saudi Arabia)	24.90	3.19	0.35	1.23	-1.5 to -1.1	0.5	-1.0	-1.2	-	[28]
Alta Floresta (Brazil)	-9.87	2.99	0.31	3.92	-1.0 to 0.0	5.2	2.4	-0.9	-	[28]
Frenchman Flat (USA)	36.80	3.54	0.07	0.89	-1.5 to -1.1	0.5	-1.1	-1.2	-	[28]
Granada (Spain)	37.15	3.56	0.15	1.27	-1.0	1.2	-0.3	-0.9	-	[28]
Beijing (China)	39.97	3.68	0.74	1.28	-1.7 to -0.8	-7.8	-4.5	-0.9	-	[28]

c-Si: crystalline silicon (m-Si and p-Si)
a-Si: amorphous silicon
CdTe: cadmium telluride
CIGS: copper indium gallium selenide
CIS: copper indium selenide
[1]Climatology taken from Fukuoka (Japan)
[2]Climatology taken from Granada (Spain)
[3]Climatology taken from Karlsruhe (Germany)
Refs. [34, 16, 17, 82]: Spectroradiometer measurements; "Spectral Factor" index calculation; section 3.2.1.1,1. Eq. (6).
Ref. [57]: Spectroradiometer measurements; "Integrated Electric Charge" index calculation; section 3.2.1.1.5, Eq. (33).
Ref. [28]: Spectra simulated with SMARTS from AERONET data; "Spectral Factor" index calculation; section 3.2.1.1.1, Eq. (6).

Table 5
Estimated relative annual average spectral impact for different HCPV technologies in percentage.

Location	Latitude (º)	AM	AOD	PW (cm)	LM+PMMA	LM+SOG	MM+PMMA	MM+SOG	Reference

Solar Village (Saudi Arabia)	24.90	3.19	0.35	1.23	-6.6	-5.1	-5.2	-3.9	[28]
Alta Floresta (Brazil)	-9.87	2.99	0.31	3.92	-4.8	-3.9	-5.2	-4.4	[28]
Frenchman Flat (USA)	36.80	3.54	0.07	0.89	-7.0	-5.7	-5.6	-4.3	[28]
Granada (Spain)	37.15	3.56	0.15	1.27	-7.3	-5.8	-6.0	-4.5	[28]
Beijing (China)	39.97	3.68	0.74	1.28	-30.6	-28.7	-28.6	-26.5	[28]
Madrid (Spain)	40.39	3.69	0.10	1.25	-5.8*		-	-	[70]

LM+PMMA: Lattice-matched GaInP/GaInAs/Ge with poly(methylmethacrylate) Fresnel lens
LM+SOG: Lattice-matched GaInP/GaInAs/Ge with silicon-on-glass Fresnel lens
MM+PMMA: Metamorphic-mismatched GaInP/GaInAs/Ge with poly(methylmethacrylate) Fresnel lens
MM+SOG: Metamorphic-mismatched GaInP/GaInAs/Ge with silicon-on-glass Fresnel lens
*Spectral losses for a Lattice-matched GaInP/GaInAs/Ge solar cell without considering optical devices.
Ref. [28]: Spectra simulated with SMARTS from AERONET data; “Spectral Factor for HCPV” index calculation; section 3.2.1.2.1, Eq. (38).
Ref. [70]: Spectroheliometer measurements; “Spectrally Corrected Direct Normal Irradiance” index calculation; section 3.2.1.2.2, Eqs. (44, 47).

5. Conclusions

The proposed classification of spectral indexes gathers and systematizes all the relevant methods for the spectral analysis available in the literature. An in depth discussion of the main features of the different procedures used by each author and/or research centre is conducted. This work can then serve as a guide and is intended to be a reference framework for future studies in this field.

The spectral indexes were classified into three categories: indexes that characterize the spectrum, indexes that characterize the spectral impact on a PV device and indexes that characterize the relative spectral impact between two PV devices. The indexes that characterize the spectrum are the average photon energy (APE) and the blue fraction (BF). The indexes that characterize the spectral impact on a PV device are: for non-concentrating PV devices, the spectral factor (SF), the spectrally corrected global irradiance (G_c), the spectral enhancement factor (SEF), the useful fraction (UF), the integrated electric charge (Q) and the spectrally effective responsivity (S_{ef}); and for HCPV devices, the spectral factor for HCPV (SF_{HCPV}) and the spectrally corrected direct normal irradiance (B_c). The indexes that characterize the relative spectral impact between two PV devices are: for non-concentrating PV devices, the spectral mismatch factor (MM); and for HCPV devices, the spectral matching ratio (SMR) and the Z-parameter (Z).

The analysis of the available methods showed that the choice of a suitable index depends on the specific application and its context. We identified four key factors to be evaluated before the selection of a spectral characterization method: the analysed PV technology, the required instruments, the availability of information on PV device spectral response and the required accuracy. For non-concentrating PV devices, SF and G_c allow an accurate spectral characterization if a spectroradiometer, a reference pyranometer and information on the device spectral response are available. SEF can be used as an alternative with lower computational effort, while MM allows replacing the pyranometer by a reference PV device. If the spectral response data is not available, UF can be used assuming a loss in accuracy. If a reference pyranometer is not available, Q or S_{ef} can be calculated. If the spectroradiometer is not available, there is the option of monitoring the short-circuit current and correcting it in temperature and angle-of-incidence in order to obtain SF, G_c or Q. For concentrating PV devices, SF_{HCPV} and B_c can provide a good approximation to the spectral gains or losses with the use of a spectroradiometer, a reference pyrheliometer and knowledge of the spectral response and optical efficiency functions. The spectroradiometer can be avoided by monitoring the short-circuit current, but noise in the measurements caused by the sun tracker motion and by temperature changes will reduce the accuracy. A practical way to approximate spectral gains or losses in these devices is the use of a spectroheliometer through indexes like Bc, SMR or Z. Finally, in all cases, there are device-independent methods (APE and BF) which can be used ignoring physical characteristics of the analysed devices, with the drawback of a lower accuracy.As a conclusion, every method presents advantages and disadvantages and it is not easy to decide between them. This paper can contribute to facilitate this task. Table 2 is a useful summary of the requirements of each of the analysed methods.

The outcome of the analysis of the impact of the spectral variations on the energy harvesting of photovoltaic systems leads to additional important conclusions. On the one hand, the PV materials

with a wide absorption band, low energy gap, have proved a stable and low spectral dependence. Because of this, they are more convenient materials to ensure a reasonable spectral behaviour and diminish as much as possible the uncertainty in the design and/or evaluation of photovoltaic facilities when is not possible or desirable to perform spectral analyses. Moreover, they are a more suitable selection if a stable seasonal system performance is required. On the other hand, the PV materials with a low abortion band, high energy gap, have shown a notable spectral dependence. In this case, spectral analyses seem mandatory in any photovoltaic system formed by these devices in order to avoid failed installations for spectral concerns and to maximize the productivity. Furthermore, these materials are good candidates for successful installations at locations dominated by a blue-rich spectral irradiance due to their remarkable annual spectral gains. Finally, HCPV systems have demonstrated to be strongly affected by the varying spectral distribution. This high spectral dependence could lead to an important reduction of the expected productivity at sites with a not suitable spectral sunlight distribution. Bearing this in mind, the accomplishment of spectral studies becomes critical for the case of this technology. For instance, locations with red-rich spectral irradiance, either by high latitudes and/or extreme AOD values, are not recommended to avoid failed HCPV facilities.

Acknowledges

Eduardo F. Fernández acknowledges the Spanish Ministry of Economy and Competitiveness for the Juan de la Cierva 2013 and 2015 fellowships. The authors also thank the Spanish Ministry of Economy and Competitiveness and FEDER funds for the projects ENE2013-45242-R and ENE2016-78251-R, and the "Plan de Apoyo a la Investigación de la Universidad de Jaén y la Caja Rural de Jaén" (UJA2015/07/01).

The authors would like to acknowledge the International AERONET Federation for providing the aerosol optical depth and precipitable water data used in this study.

References

[1] P. Faine, S. Kurtz, C. Riordan and J. M. Olson, "The influence of spectral solar irradiance variations on the performance of selected single-junction and multi-junctions solar cells," *Solar Cells,* vol. 31, pp. 259 - 278, 1991.

[2] R. E. Bird, R. L. Hulstrom and L. J. Lewis, "Terrestrial solar spectral data sets," *Solar Energy,* vol. 30, no. 6, pp. 563-573, 1983.

[3] R. Hulstrom, R. Bird y C. Riordan, «Spectral solar irradiance data sets for selected terrestrial conditions,» *Solar Cells,* vol. 15, nº 4, pp. 365-391, 1985.

[4] C. Gueymard, D. Myers y K. Emery, «Proposed reference irradiance spectra for solar energy systems testing,» *Solar Energy,* vol. 73, nº 6, pp. 443-467, 2002.

[5] ASTM G 173-03 (ed. 1), *Standard tables for reference solar spectral irradiance: direct normal and hemispherical on 37 tilted surface,* 2012.

[6] S. Philipps, G. Peharz, R. Hoheisel, T. Hornung, N. Al-Abbadi, F. Dimroth y A. Bett, «Energy harvesting efficiency of III-V triple-junction concentrator solar cells under realistic spectral conditions,» *Solar Energy Materials and Solar Cells,* vol. 94, nº 5, pp. 869-877, 2010.

[7] T. Ishii, K. Otani and T. Takashima, "Effects of solar spectrum and module temperature on outdoor performance of photovoltaic modules in round-robin measurements in Japan," *Progress in Photovoltaics: Research and Applications,* vol. 19, pp. 141-148, 2011.

[8] T. Ishii, K. Otani, T. Takashima and Y. Xue, "Solar spectral influence on the performance of photovoltaic (PV) modules under fine weather and cloudy weather conditions," *Progress in Photovoltaics: Research and Applications,* vol. 21, pp. 481-489, 2013.

[9] T. Minemoto, M. Toda, S. Nagae, M. Gotoh, A. Nakajima, K. Yamamoto, H. Takakura and Y. Hamakawa, "Effect of spectral irradiance distribution on the outdoor performance of amorphous Si//thin-film crystalline Si stacked photovoltaic modules," *Solar Energy Materials and Solar Cells,* vol. 91, pp. 120-122, 2007.

[10] T. Minemoto, S. Nagae and H. Takakura, "Impact of spectral irradiance distribution and temperature on the outdoor performance of amorphous Si photovoltaic modules," *Solar Energy Materials and Solar Cells,* vol. 91, pp. 919-923, 2007.

[11] S. Nagae, M. Toda, T. Minemoto, H. Takakura and Y. Hamakawa, "Evaluation of the impact of solar spectrum and temperature variations on output power of silicon-based photovoltaic modules," *Solar Energy Materials and Solar Cells,* vol. 90, pp. 3568-3575, 2006.

[12] S. Senthilarasu, E. F. Fernández, F. Almonacid and T. K. Mallick, "Effects of spectral coupling on perovskite solar cells under diverse climatic conditions," *Solar Energy Materials and Solar Cells,* vol. 133, pp. 92-98, 2015.

[13] E. F. Fernández, F. Almonacid, T. K. Mallick and S. Senthilarasu, "Effect of spectral irradiance variations on the performance of highly efficient environment-friendly solar cells," *IEEE Journal of Photovoltaics,* vol. 5, no. 4, pp. 1150-1157, 2015.

[14] K. Araki y M. Yamaguchi, «Influences of spectrum change to 3-junction concentrator cells,» *Solar Energy Materials and Solar Cells,* vol. 75, nº 3-4, pp. 707-714, 2003.

[15] E. F. Fernández, F. Almonacid, J. A. Ruiz-Arias and A. Soria-Moya, "Analysis of the spectral variations on the performance of high concentrator photovoltaic modules operating under

different real climate conditions," *Solar Energy Materials and Solar Cells,* vol. 127, pp. 179-187, 2014.

[16] M. Alonso-Abella, F. Chenlo, G. Nofuentes and M. Torres-Ramírez, "Analysis of spectral effects on the energy yield of different PV (photovoltaic) technologies: The case of four specific sites," *Energy,* vol. 67, pp. 435-443, 2014.

[17] D. Dirnberger, G. Blackburn, B. Müller and C. Reise, "On the impact of solar spectral irradiance on the yield of different PV technologies," *Solar Energy Materials and Solar Cells,* vol. 132, pp. 431-442, 2015.

[18] F. Kasten and A. T. Young, "Revised optical air mass tables and approximation formula," *Applied Optics,* vol. 28, no. 22, pp. 4735-4738, 1989.

[19] C. Gueymard, "Direct solar transmittance and irradiance predictions with broadband models. Part I: Detailed theoretical performance assessment," *Solar Energy,* vol. 74, no. 5, pp. 355-379, 2003.

[20] Y. A. Eltbaakh, M. Ruslan, M. Alghoul, M. Othman, K. Sopian and T. Razykov, "Solar attenuation by aerosols: An overview," *Renewable and Sustainable Energy Reviews,* vol. 16, no. 6, pp. 4264-4276, 2012.

[21] C. Gueymard, "Impact of on-site atmospheric water vapor estimation methods on the accuracy of local solar irradiance predictions," *Solar Energy,* vol. 101, pp. 74-82, 2014.

[22] J. A. Ruiz-Arias and C. A. Gueymard, "Solar Resource for High-Concentrator Photovoltaic Applications," in *High Concentrator Photovoltaics: Fundamentals, Engineering and Power Plants. Eds. Pérez-Higueras, P.; Fernández, Eduardo F.*, Springer, 2015, pp. 261-302.

[23] M. Iqbal, An Introduction to Solar Radiation, Academic Press (Canada), 1983.

[24] K. N. Liour, An Introduction to Atmospheric Radiation, Academic Press (California), 2002.

[25] N. Chan, H. Brindley and N. Ekins-Daukes, "Impact of individual atmospheric parameters on CPV system power, energy yield and cost of energy," *Progress in Photovoltaics: Research and Applications,* vol. 22, no. 10, p. 1080–1095, 2014.

[26] C. Osterwald, K. Emery and M. Muller, "Photovoltaic module calibration value versus optical air mass: The air mass function," *Progress in Photovoltaics: Research and Applications,* vol. 22, no. 5, pp. 560-573, 2014.

[27] C. Gueymard, "Parameterized transmittance model for direct beam and circumsolar spectral irradiance," *Solar Energy,* vol. 71, no. 5, pp. 325-346, 2001.

[28] E. F. Fernández, A. Soria-Moya, F. Almonacid and J. Aguilera, "Comparative assessment of the spectral impact on the energy yield of high concentrator and conventional photovoltaic technology," *Solar Energy Materials and Solar Cells,* vol. 147, pp. 185-197, 2016.

[29] C. Jardine, T. Betts, R. Gottschalg, D. G. Infield and K. Lane, "Influence of spectral effects on the performance of multijunction amorphous silicon cells," in *17th European Photovoltaic Solar Energy Conference*, München, Germany, 2002.

[30] S. Williams, T. Betts, T. Helf, R. Gottschalg, H. G. Beyer and D. G. Infield, "Modelling long-term module performance based on realistic reporting conditions with consideration to spectral effects," in *3rd World Conference on Photovoltaic Energy Conversion*, Osaka, Japan, 2003.

[31] T. Minemoto, Y. Nakada, H. Takahashi and H. Takakura, "Uniqueness verification of solar spectrum index of average photon energy for evaluating outdoor performance of photovoltaic modules," *Solar Energy,* vol. 83, pp. 1294-1299, 2009.

[32] M. Norton, A. M. Gracia-Amillo and R. Galleano, "Comparison of solar spectral irradiance measurements using the average photon energy parameter," *Solar Energy,* vol. 120, pp. 337-344, 2015.

[33] C. A. Gueymard, "Daily spectral effects on concentrating PV solar cells as affected by realistic aerosol optical depth and other atmospheric conditions," in *SPIE - Optical Modeling and Measurements for Solar Energy Systems III*, San Diego, CA, 2009.

[34] T. Ishii, K. Otani, A. Itagaki and K. Utsunomiya, "A simplified methodology for estimating solar spectral influence on photovoltaic energy yield using average photon energy," *Energy Science and Engineering,* vol. 1, no. 1, pp. 18-26, 2013.

[35] M. Hofmann, P. Vanicek and R. Haselbuhn, "Is the average photon energy (APE) a suitable measure to describe the uniqueness of solar spectra?," in *29th European Photovoltaic Solar Energy Conference*, Amsterdam, Netherlands, 2014.

[36] Y. Nakada, S. Fukushige, T. Minemoto and H. Takakura, "Seasonal variation analysis of the outdoo rperformance of amorphous Si photovoltaic modules using the contour map," *Solar Energy Materials and Solar Cells,* vol. 93, pp. 334-337, 2009.

[37] T. Minemoto, S. Fukushige and H. Takakura, "Difference in the outdoor performance of bulk and thin-film silicon-based photovoltaic modules," *Solar Energy Materials and Solar Cells,* vol. 93, pp. 1062-1065, 2009.

[38] T. Minemoto, H. Takahashi, Y. Nakada and H. Takakura, "Outdoor performance evaluation of photovoltaic modules using contour plots," *Current Applied Physics,* vol. 10, pp. 5257-5260, 2010.

[39] N. Katsumata, Y. Nakada, T. Minemoto and H. Takakura, "Estimation of irradiance and outdoor performance of photovoltaic modules by meteorological data," *Solar Energy Materials and Solar Cells,* vol. 95, pp. 199-202, 2011.

[40] C. Cornaro and A. Andreotti, "Influence of Average Photon Energy index on solar irradiance characteristics and outdoor performance of photovoltaic modules," *Progress in Photovoltaics: Research and Applications,* vol. 21, pp. 996-1003, 2013.

[41] G. Nofuentes, B. García-Domingo, M. Fuentes, R. Moreno, C. Cañete, M. Sidrach-de-Cardona, M. A. Alonso and F. Chenlo, "Comparative analysis of the effects of spectrum and module temperature on the performance of thin film modules on different sites," in *27th European Photovoltaic Solar Energy Conference*, Frankfurt, Germany, 2012.

[42] G. Nofuentes, B. García-Domingo, J. V. Muñoz and F. Chenlo, "Analysis of the dependence of the spectral factor of some PV technologies on the solar spectrum distribution," *Applied Energy,* vol. 113, pp. 302-309, 2014.

[43] A. M. Gracia-Amillo, T. Huld, P. Vourlioti, R. Müller and M. Norton, "Application of satellite-based spectrally-resolved solar radiation data to PV performance studies," *Energies,* vol. 8, pp. 3455-3488, 2015.

[44] H. Al Husna, N. Shibata, N. Sawano, S. Ueno, Y. Ota, T. Minemoto, K. Araki and K. Nishioka, "Impact of spectral irradiance distribution and temperature on the outdoor performance of concentrator photovoltaic system," *AIP Conference Proceedings,* vol. 1556, pp. 252-255, 2013.

[45] B. García-Domingo, C. J. Carmona, A. J. Rivera-Rivas, M. J. del Jesús and J. Aguilera, "A differential evolution proposal for estimating the maximum power delivered by CPV modules under real outdoor conditions," *Expert Systems with Applications,* vol. 42, no. 13, pp. 5452-5462, 2015.

[46] N. Kataoka, S. Yoshida, S. Ueno and T. Minemoto, "Evaluation of solar spectral irradiance distribution using an index from a limited range of the solar spectrum," *Current Applied Physics,* vol. 14, pp. 731-737, 2014.

[47] J. Sutterlueti, S. Ransome, R. Kravets and L. Schreier, "Characterising PV modules under outdoor conditions: what´s most important for energy yield," in *26th European Photovoltaic Solar Energy Conference and Exhibition*, Hamburg, 2011.

[48] IEC 60904-7 (Ed. 3.0), *Photovoltaic devices - Part 7: Computation of the spectral mismatch correction for measurements of photovoltaic devices,* 2008.

[49] C. J. Hibberd, F. Plyta, C. Monokroussos, M. Bliss, T. R. Betts and R. Gottschalg, "Voltage-dependent quantum efficiency measurements of amorphous silicon multi-junction mini-modules," *Solar Energy Materials and Solar Cells,* vol. 95, no. 1, pp. 123-126, 2011.

[50] C. Monokroussos, M. Bliss, Y. N. Qiu, C. J. Hibberd, T. R. Betts, A. N. Tiwari and R. Gottschalg, "Effects of spectrum on the power rating of amorphous silicon photovoltaic devices," *Progress in Photovoltaics: Research and Applications,* vol. 19, no. 6, pp. 640-648, 2011.

[51] S. Nann and K. Emery, "Spectral effects on PV-device rating," *Solar Energy Materials and Solar Cells,* vol. 27, pp. 189-216, 1992.

[52] J. J. Pérez-López, F. Fabero and F. Chenlo, "Experimental solar spectral irradiance until 2500 nm: Results and influence on the PV conversion of different materials," *Progress in Photovoltaics: Research and Applications,* vol. 15, pp. 303-315, 2007.

[53] F. Fabero, N. Vela and F. Chenlo, "Influence ofsolar spectral variations on the conversion efficiency of a-Si and m-Si PV devices: a yearly and hourly study," in *13th European Photovoltaic Solar Energy Conference*, Nice, France, 1995.

[54] R. Gottschalg, D. G. Infield and M. J. Kearney, "Experimental study of variations of the solar spectrum of relevance to thin film solar cells," *Solar Energy Materials and Solar Cells,* vol. 79, pp. 527-537, 2003.

[55] R. Gottschalg, T. R. Betts, D. G. Infield and M. J. Kearney, "The effect of spectral variations on the performance parameters of single and double junction amorphous silicon solar cells," *Solar Energy Materials and Solar Cells,* vol. 85, pp. 415-428, 2005.

[56] R. Gottschalg, T. R. Betts, D. G. Infield and M. J. Kearney, "On the importance of considering the incident spectrum when measuring the outdoor performance of amorphous silicon photovoltaic devices," *Measurement Science and Technology,* vol. 15, pp. 460-466, 2004.

[57] B. Zinsser, M. B. Schubert and J. H. Werner, "Spectral dependent annual yield of different photovoltaic technologies," in *26th European Photovoltaic Solar Energy Conference*, Hamburg, Germany, 2011.

[58] N. Martín and J. M. Ruiz, "A new method for the spectral characterisation of PV modules," *Progress in Photovoltaics: Research and Applications,* vol. 7, pp. 299-310, 1999.

[59] A. Soria-Moya, E. F. Fernández, F. Almonacid and T. K. Mallick, "Spectral losses of high concentrator photovoltaic modules depending on latitude," *AIP Conference Proceedings,* vol. 1679, no. 1, pp. 1-7, 2015.

[60] T. Hornung, M. Steiner and P. Nitz, "Estimation of the influence of Fresnel lens temperature on energy generation of a concentrator photovoltaic system," *Solar Energy Materials and Solar Cells,* vol. 99, pp. 333-338, 2012.

[61] H. Baig, K. Heasman and T. K. Mallick, "Non-uniform illumination in concentrating solar cells," *Renewable and Sustainable Energy Reviews,* vol. 16, pp. 5890-5909, 2012.

[62] E. F. Fernández, F. Almonacid, A. Soria-Moya and J. Terrados, "Experimental analysis of the spectral factor for quantifying the spectral influence on concentrator photovoltaic systems under real operating conditions," *Energy,* vol. 90, pp. 1878-1886, 2015.

[63] J. Hashimoto, K. Sakurai and K. Otani, "Performance of CPV system using three types of III-V multi-junction solar cells," in *8th International Conference on Concentrating Photovoltaic Systems*, Toledo, Spain, 2012.

[64] F. Almonacid, P. J. Pérez-Higueras, E. F. Fernández and P. Rodrigo, "Relation between the cell temperature of a HCPV module and atmospheric parameters," *Solar Energy Materials and Solar Cells,* vol. 105, pp. 322-327, 2012.

[65] Y. S. Kim, S. M. Kang and R. Winston, "Tracking control of high-concentration photovoltaic systems for minimizing power losses," *Progress in Photovoltaics: Research and Applications,* vol. 22, pp. 1001-1009, 2014.

[66] M. Muller, B. Marion, S. Kurtz and J. Rodríguez, "An investigation into spectral parameters as they impact CPV module performance," in *6th International Conference on Concentrating Photovoltaic Systems*, Freiburg, Germany, 2010.

[67] E. F. Fernández and F. Almonacid, "Spectrally corrected direct normal irradiance based on artificial neural networks for high concentrator photovoltaic applications," *Energy,* vol. 74, pp. 941-949, 2014.

[68] F. Almonacid, E. F. Fernández, T. K. Mallick and P. J. Pérez-Higueras, "High concentrator photovoltaic module simulation by neuronal networks using spectrally corrected direct normal irradiance and cell temperature," *Energy,* vol. 84, pp. 336-343, 2015.

[69] I. Antón, M. Martínez, F. Rubio, R. Núñez, R. Herrero, C. Domínguez, M. Victoria, S. Askins and G. Sala, "Power rating of CPV systems based on spectrally corrected DNI," *8th*

International Conference on Concentrating Photovoltaic Systems, AIP Conference Proceedings, vol. 1477, pp. 331-335, 2012.

[70] R. Núñez, C. Domínguez, S. Askins, M. Victoria, R. Herrero, I. Antón and G. Sala, "Determination of spectral variations by means of component cells useful for CPV rating and design," *Progress in Photovoltaics: Research and Applications,* 2015.

[71] G. Peharz, J. P. Ferrer-Rodríguez, G. Siefer and A. W. Bett, "A method for using CPV modules as temperature sensors and its application to rating procedures," *Solar Energy Materials and Solar Cells,* vol. 95, pp. 2734-2744, 2011.

[72] M. Victoria, S. Askins, R. Núñez, C. Domínguez, R. Herrero, I. Antón, G. Sala and J. M. Ruiz, "Tuning the current ratio of a CPV system to maximize the energy harvesting in a particular location," *9th International Conference on Concentrating Photovoltaic Systems, AIP Conference Proceedings,* vol. 1556, pp. 156-161, 2013.

[73] R. Núñez, C. Jin, M. Victoria, C. Domínguez, S. Askins, R. Herrero, I. Antón and G. Sala, "Spectral study and classification of worldwide locations considering several multijunction solar cell technologies," *Progress in Photovoltaics: Research and Applications,* vol. DOI: 10.1002/pip.2781, 2016.

[74] C. Domínguez, I. Antón, G. Sala and S. Askins, "Current-matching estimation for multijunction cells within a CPV module by means of component cells," *Progress in Photovoltaics: Research and Applications,* vol. 21, pp. 1478-1488, 2013.

[75] B. García-Domingo, J. Aguilera, J. de la Casa and M. Fuentes, "Modelling the influence of atmospheric conditions on the outdoor real performance of a CPV (Concentrated Photovoltaic) module," *Energy,* vol. 70, pp. 239-250, 2014.

[76] G. Peharz, G. Siefer and A. W. Bett, "A simple method for quantifying spectral impacts on multi-junction solar cells," *Solar Energy,* vol. 83, pp. 1588-1598, 2009.

[77] J. Leloux, E. Lorenzo, B. García-Domingo, J. Aguilera and C. Gueymard, "A bankable method of assessing the performance of a CPV plant," *Applied Energy,* vol. 118, pp. 1-11, 2014.

[78] D. Talavera, P. Pérez-Higueras, J. Ruíz-Arias y E. Fernández, «Levelised cost of electricity in high concentrated photovoltaic grid connected systems: Spatial analysis of Spain,» *Applied Energy,* vol. 151, pp. 49-59, 2015.

[79] E. Fernández, P. Pérez-Higueras, F. Almonacid, J. Ruiz-Arias, P. Rodrigo, J. Fernandez and I. Luque-Heredia, "Model for estimating the energy yield of a high concentrator photovoltaic system," *Energy,* vol. 87, pp. 77-85, 2015.

[80] E. Fernández, D. Talavera, F. Almonacid y G. Smestad, «Investigating the impact of weather variables on the energy yield and cost of energy of grid-connected solar concentrator systems,» *Energy,* vol. 106, pp. 790-801, 2016.

[81] B. Holben, T. Eck, I. Slutsker, D. Tanré, J. Buis, A. Setzer, E. Vermote, J. Reagan, Y. Kaufman, T. Nakajima, F. Lavenu, I. Jankowiak and A. Smirnov, "AERONET - A federated instrument network and data archive for aerosol characterization," *Remote Sensing of Environment,* vol. 66, no. 1, pp. 1-16, 1998.

[82] J. Y. Ye, T. Reindl, A. G. Aberle and T. M. Walsh, "Effect of solar spectrum on the performance of various thin-film PV module technologies in tropical Singapore," *IEEE Journal of Photovoltaics,* vol. 4, no. 5, pp. 1268-1274, 2014.